LA-9602-MS

2

Los Alamos National Laboratory is operated by the University of California for the United States Department of Energy under contract W-7405-ENG-36.

...icient Methods for Time Absorption ...) Eigenvalue Calculations

Los Alamos Los Alamos National Laboratory
Los Alamos, New Mexico 87545

LA-9602-MS

UC-32
Issued: March 1983

Efficient Methods for Time Absorption (α) Eigenvalue Calculations

Thomas R. Hill

Los Alamos National Laboratory
Los Alamos, New Mexico 87545

CONTENTS

EFFICIENT METHODS FOR TIME ABSORPTION (α) EIGENVALUE CALCULATIONS

by

Thomas R. Hill

ABSTRACT

The time-absorption eigenvalue calculation represents one of the options found in most discrete-ordinates transport codes. This report describes several methods developed at Los Alamos to improve the efficiency of this calculation. Two procedures, based on coarse mesh rebalance, to accelerate the α eigenvalue iterations are derived. Some simple modifications to the iteration convergence precisions and the iteration strategy reduce the number of unnecessary calculations in the early stages of the problem. A procedure to prevent code failures on α searchs for subcritical systems is detailed. For the test problems examined, these methods resulted in convergence with one-fifth the number of iterations required for the standard eigenvalue search procedure.

I. INTRODUCTION

The time-absorption (α) eigenvalue is one of the implicit eigenvalue search options found in most current transport codes.[1-5] Because these codes are designed to treat a variety of implicit eigenvalue problems (critical size search, concentration search), their generalized search methods are less than optimal

for a specific type of eigenvalue calculation. Due to the explicit nature of the α eigenvalue problem and the types of nuclear systems of interest at Los Alamos, a number of methods have been developed to considerably improve the efficiency of these codes for this eigenvalue search. This report describes these methods.

We will start with the homogeneous, time- and energy-dependent, transport equation

$$\frac{1}{v}\frac{\partial\psi}{\partial t} + \nabla\cdot\vec{\Omega}\psi + \Sigma_t(\vec{r},E)\,\psi(\vec{r},E,\vec{\Omega},t) = \int dE' \int d\vec{\Omega}'\, \Sigma_s(\vec{r},E'\to E,\vec{\Omega}\cdot\vec{\Omega}')\,\psi(\vec{r},E',\vec{\Omega}',t)$$

$$+ \chi(E)\int dE' \int d\vec{\Omega}'\, \nu\Sigma_f(\vec{r},E')\,\psi(\vec{r},E',\vec{\Omega}',t) \quad , \tag{1}$$

where

$\psi(\vec{r},E,\vec{\Omega},t)$ = angular flux as a function of the independent variables time (t), energy (E) or velocity (v), angle ($\vec{\Omega}$), and space ($\vec{r}$),
$\Sigma_t(\vec{r},E)$ = macroscopic total cross section,
$\Sigma_s(\vec{r},E'\to E,\vec{\Omega}\cdot\vec{\Omega}')$ = macroscopic scattering function,
$\chi(E)$ = fission spectrum, and
$\nu\Sigma_f(\vec{r},E)$ = macroscopic prompt fission neutron production cross section.
By making the time separability ansatz

$$\psi(\vec{r},E,\vec{\Omega},t) = e^{\alpha t}\psi_\alpha(\vec{r},E,\vec{\Omega}) \quad , \tag{2}$$

Eq. (1) is transformed to a time-independent eigenvalue problem

$$L\psi_\alpha + \left(\Sigma_t + \frac{\alpha}{v}\right)\psi_\alpha = (S + F)\,\psi_\alpha \quad , \tag{3}$$

where

L = leakage operator,

S = scattering operator,

F = fission operator, and

ψ_α and α are the time-absorption eigenfunctions and eigenvalues, respectively.

There is a very rich literature[6-11] on the eigenvalue spectrum of Eq. (3). Duderstadt and Martin[11] give a particularly good discussion of this problem, with abundant references. The Larsen and Zweifel[9] article is probably the most complete and general of the recent papers.

Of particular interest is the eigensolution of Eq. (3) with the largest real part, α_0, the so-called "dominant" eigenvalue.[10] This solution corresponds to the asymptotic (as $t\to\infty$) solution of the original initial value problem, Eq. (1). This dominant eigenvalue is the physical quantity measured in the laboratory by pulsed neutron (die-away) and Rossi-α experiments. Physical consideration would obviously require

$$\mathrm{Im}(\alpha_0) = 0 \tag{4a}$$

and

$$\psi_{\alpha_0}(\vec{r},E,\vec{\Omega}) \geq 0 \quad \text{for all } \vec{r},\ E,\ \vec{\Omega} \quad . \tag{4b}$$

Also of importance is the sign of α_0

$$\alpha_0 \begin{cases} > 0 & \text{supercritical} \\ = 0 & \text{critical} \\ < 0 & \text{subcritical} \end{cases} \quad .$$

It should be noted that the α eigenfunctions of Eq. (3) differ from the λ (or k_{eff}) eigenfunctions,[6] ψ_λ, which satisfy

$$L\psi_\lambda + \Sigma_t\psi_\lambda = \left(S + \frac{1}{\lambda} F\right)\psi_\lambda \quad , \tag{5}$$

except for the exactly critical case ($\lambda = 1$ and $\alpha = 0$). The solution of Eq. (5), the k_{eff} problem, is the calculation most commonly done with steady-state transport codes. Because the α eigenvalue appears in Eq. (3) as a 1/v absorber (hence the name time absorption), the energy spectra of ψ_α and ψ_λ can differ greatly for systems far from exactly critical. Furthermore, the spatial distributions can also differ greatly. For systems far subcritical, the ψ_α eigenfunction can have a convex, downward spatial distribution, contrary to physical intuition.

For this report, it is sufficient to proceed directly to the multigroup[6,12] form of Eq. (3), written as

$$L\psi + (\Sigma_t + \alpha V^{-1})\,\psi(\vec{r},\vec{\Omega}) = (S + \frac{1}{\lambda} F)\,\psi \quad , \tag{6}$$

where $\psi(\vec{r},\vec{\Omega})$ is a vector of multigroup angular fluxes, $\psi_g(\vec{r},\vec{\Omega})$, g = 1 to IGM, and L, Σ_t, S, and F are the multigroup approximations to the corresponding operators in Eq. (3). The intermediate eigenvalue λ has been introduced and the solution, α and ψ, of Eq. (6) is sought such that $\lambda = 1$. The angular variable $\vec{\Omega}$ will be treated with the standard discrete-ordinates approximation.[12] For the schemes to be described in this report, the actual geometry and the spatial approximation used are immaterial, although the testing was done for two-dimensional geometry with a finite difference (diamond difference[12,14]) approximation of the spatial variable $\vec{r}$.

The existence of a dominant eigenvalue, α_0, for the multigroup transport Eq. (6), for finite media, under very general conditions, has been shown by Larsen.[10]

This report is organized in the following manner. Part II briefly describes the methods currently used in most current transport codes. Part III and IV outline the application of coarse mesh rebalance (CMR)[3] acceleration to the α eigenvalue search. Part V details some modifications to the iteration strategy that can improve computational efficiency. Part VI presents some numerical results for typical test problems to demonstrate the efficiencies effected by these improved methods. Finally, Part VII summarizes the mathematical literature for the α eigenvalue problem and describes a procedure to make more robust the eigenvalue search for subcritical systems, a particularly difficult calculation.

II. STANDARD METHODS

The standard iterative methods for solving the multigroup discrete-ordinates transport equation are detailed in the appropriate code manuals[1-3] and elsewhere.[12] The inner iterations for a single energy group are performed on the within-group scatter source. The outer iterations are performed on the fission source, yielding upon convergence, the intermediate eigenvalue λ of Eq. (6). For $\alpha = 0$, this λ is merely k_{eff} for the system.

The α eigenvalue problem is solved as a sequence of λ eigenvalue problems until an α for which $\lambda = 1$ is obtained. This $\underline{\alpha}$ $\underline{\text{iteration}}$ overlying the outer and inner iterations can be written as

$$L\psi^k + (\Sigma + \alpha^k v^{-1})\,\psi^k = \left(S + \frac{1}{\lambda^k} F\right)\psi^k \quad , \tag{7}$$

where k is the α iteration index. The procedure by which the next α^{k+1} is selected, based on α^k, λ^k, and ψ^k, constitutes the $\underline{\alpha}$ $\underline{\text{eigenvalue}}$ $\underline{\text{search}}$ procedure, the subject of this report.

The standard eigenvalue search procedure is roughly as follows:

1. Make an initial guess of eigenvalue α^o, usually = 0.
2. Solve the transport Eq. (7), performing inner and outer iterations until convergence, for λ^o.
3. Obtain the second guess α^1 by adjusting α^o with the $\underline{\text{eigenvalue}}$ $\underline{\text{modifier}}$ EVM

   $$\alpha^1 = \alpha^o + \text{EVM} \quad .$$

4. Solve the transport Eq. (7) for λ^1.
5. Using the points (λ^k,α^k) and $(\lambda^{k-1},\alpha^{k-1})$, perform a linear extrapolation of $\lambda(\alpha)$ to that α^{k+1} for which $\lambda^{k+1}(\alpha^{k+1}) = 1$. Or, alternatively, using the points (λ^k,α^k), $(\lambda^{k-1},\alpha^{k-1})$, and $(\lambda^{k-2},\alpha^{k-2})$, perform a quadratic extrapolation of $\lambda(\alpha)$ to that α^{k+1} for which $\lambda^{k+1}(\alpha^{k+1}) = 1$.
6. Solve the transport Eq. (7) for λ^{k+1}.
7. Repeat until $\lambda^{k+1} = 1$.

The code user is required to provide an initial eigenvalue guess α° and an eigenvalue modifier EVM. In many cases, particularly if the neutronics are coupled to a hydrodynamics calculation, the user has little idea of the value, or even the sign, of α°. The eigenvalue modifier is seldom more than a wild guess. A poor choice of EVM, either in magnitude or sign, can significantly slow the search procedure, if not, in the case of subcritical systems, cause it to fail. In the early α iterations, the root-finding procedure of step 5 can sometimes cause the α search to flounder about.

Further details of the eigenvalue search procedure are described in the code manuals.[1-3] Additional input parameters are available to make the eigenvalue search proceed more efficiently. However, seldom is enough known about a problem to permit an a priori selection of these paramaters, even by the most intelligent code users.

Because of these deficiencies in the α search procedure, it is desirable to devise an alternate procedure, one preferably based on the physics of the problem, that will produce more rapid convergence and require fewer input parameters from the code user.

III. GROUP-COLLAPSE COARSE MESH REBALANCE

The coarse mesh rebalance CMR method[1,3,12] has been found to be an efficient means of accelerating the inner and outer iterations of the transport equation solution. This method is based on integrating the transport equation over various coarse mesh spatial regions to obtain a (usually) small system of equations for rebalance factors; factors which, when used to multiply the fluxes, at the end of each iteration force the rebalanced fluxes to satisfy particle conservation over each coarse mesh zone. This procedure has been found to effect a sometimes substantial acceleration of the iterations. For most problems, the coarse mesh used for the rebalance acceleration is simply chosen to be the material mesh.

Typically, for the outer iteration acceleration, a group-collapse rebalance, obtained by summing over all energy groups, is used to obtain a matrix eigenvalue equation for the intermediate eigenvalue λ. Because the eigenvalue α appears as an explicit scalar variable in Eq (6), similar to λ, the CMR procedure can also be applied to accelerate the α iterations of Eq. (7).

To obtain the group-collapse coarse mesh rebalance (GCCMR) equations the solution of Eq. (6) is sought for the eigenvalue α with $\lambda = 1$. Multiplying the fluxes in Eq. (6) by coarse mesh dependent rebalance factors, f_k, and integrating over all angles, all energy groups (group collapse), and all mesh cells in coarse mesh zone K yields a matrix eigenvalue equation

$$[FL + AB - FS]\ f = -\alpha\ \ FV\ \ f\ \ , \tag{8}$$

of size equal to the number of coarse mesh zones KM, for the eigenvalue α and eigenvector of rebalance factors f.

The diagonal matrices AB, FS, and FV are

$$AB_K = \int_K dV \int dE\ \Sigma_a \phi = \text{absorption}\ \ , \tag{9a}$$

$$FS_K = \int_K dV \int dE\ \ \nu\Sigma_f \phi = \text{fission neutron production, and} \tag{9b}$$

$$FV_K = \int_K dV \int dE\ \ \frac{1}{v}\ \phi = \text{total neutrons.} \tag{9c}$$

Here, ϕ is the spatial and energy-dependent scalar flux and Σ_a is the macroscopic effective absorption cross section[1,3]

$$\Sigma_a\ (E) = \Sigma_t(E) - \int dE' \int d\mu_0\ \Sigma_s(E \to E', \mu_0)\ \ , \tag{10}$$

where $\mu_0 = \vec{\Omega}\cdot\vec{\Omega}'$ = scattering angle. In practice, the integrals of Eq. (9) are carried out by sums over spatial mesh cells and energy groups in the discretized space.

The coarse mesh flow matrix, FL, consists of the group-summed outflows from zone K on the diagonal and negative inflows from zone I into zone J on the off-diagonal elements:

$$FL = \begin{bmatrix} OF_1 & -IF_{2\to1} & \cdots & -IF_{KM\to1} \\ -IF_{1\to2} & OF_2 & & \\ \vdots & & \ddots & \\ -IF_{1\to KM} & & & OF_{KM} \end{bmatrix} \tag{11}$$

For one-dimensional geometries, this flow matrix will be tridiagonal. In general, for multidimensional, orthogonal and nonorthogonal meshes, it will be a full, nonsymmetric, diagonally dominant matrix. It can be noted that

$$OF_K \geq \sum_{\substack{I=1 \\ I \neq K}}^{KM} IF_{K\to I} \tag{12}$$

with the equality holding when coarse mesh zone K has no surfaces on the outer boundary. This implies the L_1 norm $||FL|| > 0$.

In general, Eq. (8) permits the existence of complex eigenvalues, necessitating the use of a generalized eigenvalue-eigenvector routine for its solution if all the eigenvalues are to be obtained. Experience on a variety of problems has shown the eigenvalue spectrum of Eq. (8) to range from negative eigenvalues, large in magnitude, occasionally in complex conjugate pairs, to a most positive, dominant eigenvalue corresponding to α_0 of Eq. (4). It can, in fact, be shown[15] that there exists a dominant eigenvalue of Eq. (8), with zero imaginary component, which corresponds to an eigenvector with entirely positive components.

Because of the large negative eigenvalues, the simple power iteration[1] which is used to solve the outer CMR equations for λ cannot be used for Eq. (8) inasmuch as it converges to the largest eigenvalue in magnitude, not the most positive one. However, the inverse power iteration[16] (Wielandt's method of fractional iteration) can be applied to obtain the dominant eigenvalue of Eq. (8). This method involves choosing some estimate of an eigenvalue and this modified power method then converges to the eigenvalue nearest that guess. By choosing an initial guess of the dominant eigenvalue sufficiently large, this inverse power iteration

will converge to that desired, most positive eigenvalue. In typical problems, this inverse power iteration is found to converge quite rapidly, usually in from 3 to 8 iterations.

The GCCMR is performed as follows: During the inner iterations for each group, when the angular flux is being calculated, the flows between each region $IF_{I\to J}$ and the outflows for each region OF_K are computed. At the completion of the inners for that group, these flows are accumulated (group-summed) into the flow array, FL. Upon convergence of the outer iterations (for a particular α guess), the three flux integrals of Eq. (9) are computed for each coarse mesh zone. The matrix Eq. (8) is then solved for a dominant eigenvalue, which will then be used as the next α guess. The rebalance factors, f, of Eq. (8) are applied to the scalar flux and moments and the next α iteration is then begun.

This GCCMR α search procedure eliminates the need for the eigenvalue modifier and the root-finding procedure of the standard method. In fact, the intermediate eigenvalue λ plays no role in this search procedure. In practice, it has been found that GCCMR gives remarkably good estimates of α for the early α iterations, but that it converges much more slowly than the root-finding procedure in the later stages. Thus, the recommended procedure is to use GCCMR for the first few (three or four) α estimates, then switch over to a root-finding procedure for the final convergence.

A simple whole system variant of the α CMR can be derived. Integrating Eq. (7) over all energy groups and all space points yields the balance equation

$$NL^k + AB^k + \alpha^k FV^k = \frac{1}{\lambda^k} FS^k \quad , \tag{13}$$

for the k'th α iteration, where NL is the total net leakage of neutrons from the system. We would like the k+1'st iteration to satisfy the balance equation with $\lambda = 1$:

$$NL^{k+1} + AB^{k+1} + \alpha^{k+1} FV^{k+1} = FV^{k+1} \quad . \tag{14}$$

Subtracting Eq. (14) from Eq. (13) and assuming $\phi^{k+1} \cong \phi^k$ (so that $NL^{k+1} \cong NL^k$, $AB^{k+1} \cong AB^k$, etc.) yield

$$\alpha^{k+1} = \alpha^k + (1 - \frac{1}{\lambda^k}) \frac{FS^k}{FV^k} \tag{15}$$

as the next estimate for the eigenvalue. Equation (8) for the case of a one-material region can be shown equivalent to Eq. (15).

The GCCMR Eq. (8) yields not only the next guess for the eigenvalue α, but also the vector of rebalance factors f which are applied to all the fluxes in each coarse mesh zone. Since the magnitude of this eigenvector is arbitrary, normalization is typically chosen to maintain a total fission neutron source of unity

$$FT = \sum_{k=1}^{KM} FS_k = 1 \quad . \tag{16}$$

At the completion of the first α iteration, the rebalance factors for the outer rebalance equation

$$[FL^0 + AB^0] \, f^0_{outer} = \frac{1}{\lambda^0} \, FS^0 f^0_{outer} \tag{17}$$

will be identically unity ($\alpha^0 = 0$ is assumed), where $\lambda^0 = k_{eff}$. The rebalance factors from the first α rebalance equation

$$[FL^0 + AB^0 - FS^0] \, f^0_\alpha = - \alpha^1 \, FV^0 f^0_\alpha \tag{18}$$

will be those coarse mesh rebalance factors that convert the spatial distribution of the k_{eff} solution fluxes to the approximate spatial distribution of the converged α eigenvalue fluxes. Clearly, these rebalance factors will differ the most from unity (and, hence, provide the most acceleration) for problems in which the α spatial distribution differs greatly from the k_{eff} spatial distribution.

This will occur for problems far removed from critical ($\alpha = 0$) and with much spatial inhomogeneity. For spatially homogeneous problems (where KM = 1), there is no acceleration from the rebalance factor ($f_\alpha^0 = 1$), only from the improved estimate of α^1. In practice, only a modest amount of the acceleration from GCCMR comes from the rebalance factors; most of the acceleration comes from the improved estimates of α. For a typical test problem (#4) described in Part VI, which contains considerable spatial structure, these rebalance factors for f_α^0 ranged from 1.43 in the innermost material zone, to 0.25 in the outermost zone.

IV. WHOLE SYSTEM GROUPWISE REBALANCE

The α eigenvalue appears in Eq. (3) as a 1/v absorber. For problems with many energy groups and a broad range of neutron speeds, the α eigenvalue can greatly change the spectral distribution from the k_{eff} solution. This suggests a rebalance that does <u>not</u> integrate out the energy dependence (no group collapse), but that maintains a groupwise dependence, might provide an effective α acceleration.

One such procedure would be to eliminate the integration over all energies in deriving the CMR equations in Part III. This would yield a matrix equation of size KM*IGM, the number of coarse mesh regions times the number of energy groups. For many problems, this can be of size 50 to 100 or larger, resulting in a rather large rebalance equation to be solved, and greatly increasing the usually negligible overhead to perform the rebalance acceleration.

A second, more feasible, procedure to obtain rebalance equations would be to eliminate the integration over all energy groups, but integrate over all space, rather than each coarse mesh zone. This whole system groupwise rebalance (WSGR) matrix equation will be only of size IGM, the number of energy groups.

To obtain the WSGR equations, we start with the transport equation, Eq. (6) for one energy group g with the condition of $\lambda = 1$

$$L\psi_g + (\Sigma_t + \frac{\alpha}{v_g})\,\psi_g(\vec{r},\vec{\Omega}) = \sum_{g'=1}^{g} \Sigma_{sg'\to g}\,\phi_{g'} + \chi_g \sum_{g'=1}^{IGM} \nu\Sigma_{fg'}\phi_{g'} \quad . \qquad (19)$$

In Eq. (19) we have assumed no upscattering, although the method can just as easily treat problems with upscatter. Multiplying the fluxes in Eq. (19) by groupwise dependent rebalance factors, f_g, and integrating over all angles and all mesh cells yields the WSGR matrix eigenvalue equation

$$[NL + C - S - FS]\ f = -\alpha\ FV\ f \quad , \tag{20}$$

of size equal to the number of energy groups IGM, for the eigenvalue α and the eigenvector of rebalance factors f.

The diagonal matrices NL, C, and FV are

NL_g = net leakage from the system for group g, (21a)

$C_g = \int dV\ \Sigma_{tg}\phi_g$ = within-group total collision rate in group g, and (21b)

$FV_g = \int dV\ \frac{1}{v_g}\ \phi_g$ = total neutrons in group g. (21c)

Again, in practice, the integrals over all space in Eq. (21) are carried out as sums over spatial-mesh cells in the discretized space. The lower triangular (for downscatter only) matrix S of group-to-group scattering rates is of the form

$$[S] = \begin{bmatrix} \int dV\Sigma_{1\to1}\phi_1 & & \bigcirc \\ \int dV\Sigma_{1\to2}\phi_1 & \int dV\Sigma_{2\to2}\phi_2 & \\ \int dV\Sigma_{1\to IGM}\phi_1 & \int dV\Sigma_{2\to IGM}\ \phi_2 & \int dV\Sigma_{IGM\to IGM}\phi_{IGM} \end{bmatrix} \tag{21d}$$

or

$$[S_{gg'}] = [\int dV\Sigma_{g'\to g}\phi_{g'}] \quad . \tag{21d}$$

The full matrix FS of fission production rates is of the form

$$[FS] = \begin{bmatrix} \chi_1 & & \\ & \chi_2 & \\ & & \chi_{IGM} \end{bmatrix} \begin{bmatrix} \int dV\nu\Sigma_{f1}\phi & \int dV\nu\Sigma_{f2}\phi_2 & \cdots & \int dV\nu\Sigma_{fIGM}\phi_{IGM} \\ \vdots & \vdots & & \vdots \end{bmatrix} , \quad (21e)$$

or

$$[FS_{gg'}] = [\chi_g \int dV\nu\Sigma_{fg'}\phi_{g'}] \quad . \quad (21e)$$

For one-group problems, Eq. (20) can be shown identical to Eq. (15). As in GCCMR, the nonsymmetry of Eq. (20) admits complex eigenvalues. Test calculations have shown the eigenvalue spectrum ranges from negative eigenvalues, large in magnitude, occasionally in complex conjugate pairs, to the most positive, dominant eigenvalue, corresponding to α_0. By the same proof as for GCCMR[15], the existence of a dominant eigenvalue, with zero imaginary component, corresponding to a eigenvector with entirely positive components, can be shown. Implementation of the WSGR is done exactly as the GCCMR, with the inverse power iteration being used to solve Eq. (20) for the dominant eigenvalue.

For a typical test problem (#4) described in Part VI, with 12 energy groups, the rebalance factors of Eq. (20) range from 2.27 for the first group down to 1.56×10^{-5} for the bottom group, indicating that a large spectral effect is, in fact, present.

Between the two α rebalance schemes, GCCMR or WSGR, it is not clear, a priori, which is the better. In practice, the scheme of choice is found to be problem dependent. Since most code users would seldom have the knowledge to correctly choose between the two schemes, this suggests that a hybrid rebalance scheme, using first GCCMR and then WSGR, might have some merit. Since convergence of the $\alpha^n \to \alpha_0$ is often monotonic in the early α iterations, the next α guess can be chosen (from between the two different rebalance α's) to produce the largest change from the current α guess. However, both sets of rebalance factors, from GCCMR and WSGR, can be applied to the scalar flux and moments. By using both

sets of rebalance factors, it is hoped that a serendipitous acceleration of the α iterations is achieved. In practice, this does not occur and the hybrid rebalance merely results in the most effective rebalance scheme being automatically used.

V. VARIABLE CONVERGENCE PRECISION AND ITERATION STRATEGIES

In this section, we discuss some of the modifications to the iteration strategy that can be made to improve the overall efficiency of the calculation.

The standard method for α eigenvalue problems consists of a set of λ (or k_{eff}) eigenvalue problems and use of a root-finding procedure, linear or quadratic, to estimate, usually by an extrapolation, the next α guess. Because the root-finding procedure can often lead to wild extrapolations, especially for subcritical systems, it is important that each λ calculation be fully converged.

If a rebalance method, as opposed to a root-finding method, is utilized to provide the next α estimate, it may be possible to converge rather loosely the early λ calculations, when the estimate of α is poor, inasmuch as the rebalance is a function only of the fluxes.

One scheme for permitting a loose convergence early in the α calculation is termed "variable convergence precision". In typical discrete-ordinates transport codes, there are several different convergence precisions, fixed at the start of the calculation, that are used to determine convergence of the various iterations. Two of these convergence precisions are on the inner iterations, ε_i, so that

$$\max_{ij} \frac{\left|\phi^{\ell}_{ijg} - \phi^{\ell-1}_{ijg}\right|}{\phi^{\ell}_{ijg}} \leq \varepsilon_i \quad , \tag{22a}$$

where ℓ = inner iteration index, ij = spatial mesh index; and on the outer iterations, ε_o, so that

$$|\lambda^n - \lambda^{n-1}| \leq \varepsilon_0 \tag{22b}$$

where n = outer iteration index. The α calculation is continued until the final convergence test is satisfied.

$$|\lambda^k - 1| \leq \varepsilon_{final} \quad , \tag{22c}$$

where k is the α iteration index and ε_{final} is the user-specified overall convergence precision.

The "variable convergence precision" scheme consists of allowing the two intermediate convergence precisions to vary through the course of the α calculation, making them relatively large at the start of the problem, when α is poorly known (and, therefore, λ far from unity), and tightening them up as the calculation approaches convergence. One simple, ad hoc scheme to do this is to choose

$$\varepsilon_i^k = \varepsilon_0^k = 0.1 \, |1 - \lambda^k| + \lambda \, \varepsilon_{final} \quad . \tag{23}$$

By this prescription, the early inner and outer iterations are converged to a precision of the order 0.1 and, as $\lambda \to 1$, the two iterations are eventually converged to the desired precision, ε_{final}.

For many typical α eigenvalue problems, the first few α iterations, where the changes in α are the greatest, require the most outer iterations on the eigenvalue λ, despite the looser convergence precision allowed by Eq. (23). Another method for avoiding wasted iterations in the early part of the α calculation is to impose an outer iteration limit on each α iteration. By allowing only a few outer iterations before making a new α guess, many of these wasted early outers can be eliminated. In practice, an outer iteration limit per α iteration of 4 or 5 has been found to be near optimal. Fewer than that does not permit a great enough change in the flux to produce a very large change in α except for the very early iterations.

Furthermore, since the α rebalance acceleration requires only the scalar flux (but not λ) and is quite inexpensive to perform, it is possible to do an α rebalance at the completion of each outer iteration. The rebalance schemes are found to give surprisingly good estimates of α even with these very inaccurate fluxes.

The most effective iteration strategy is thus found to be the following steps:

1. Perform two α iterations, doing only one outer iteration per α iteration, and using rebalance to estimate the next α.
2. Increase the outer iteration limit to five, perform the outer iterations to obtain an estimate of λ, and then use the fluxes from this α iteration for one last rebalance estimate of α.
3. Maintaining an outer iteration limit of five, perform outer iterations, and use the linear (or quadratic) root-finding procedure for subsequent estimates of α.

It should be pointed out that these procedures of allowing a very loose convergence early in the calculation, when coupled to the root-finding α search procedure from the start (as is done in present transport codes), can reduce the robustness of the iteration process. For fast supercritical assemblies, highly absorbing and fission dominated, this is generally not a problem. It is more likely to occur for thermal reactor systems where scattering dominates, in the bottom energy group and convergence is typically slow. But, when done in conjunction with the rebalance α search method, the loose convergence procedure has not appeared to reduce the robustness of the iterations.

VI. TEST PROBLEMS AND RESULTS

In this section, we will apply the schemes developed in Parts III-V to five different test problems to demonstrate the efficiencies achieved.

The schemes were developed and implemented in the arbitrary Lagrangian mesh transport code LaMEDOC,[14] although the test problems used were entirely one-dimensional. The coding for the rebalance schemes is detailed in the Appendix. It was found that the overhead for performing both the α rebalance accelerations was negligible. Thus, the comparison of the schemes is based merely on the total number of inner iterations required for convergence, the actual computation time being proportional to that figure. All calculations were performed in the S_2P_0 approximation.

The various computational schemes used are described as follows:

Scheme STD: This is the standard search procedure used in typical transport codes, as described in Part II, including the root-finding α search. Convergence precision on inner and outer iterations

is the code default, 10^{-4}. An inner iteration limit of 25 is included but no limit on the outer iterations. The overall problem is considered converged when $|1-\lambda^n| \leq 10^{-4}$. By an appropriate choice of the eigenvalue modifier, EVM, the standard procedure can be made to look as good or as bad as desired. In these problems, the code default of EVM = 0.01 gen/shake (1 shake = 10^{-8} s) is used.

Scheme VCP: This is the variable convergence precision scheme, as described in Part V. The α eigenvalue search procedure is the same as in the STD scheme. The inner iteration limit of 25, with no outer iteration limit, is maintained.

Scheme GCCMR: This is the group-collapse coarse mesh rebalance scheme, described in Part III, which is applied to the α eigenvalue search. The GCCMR is used only for the first three α guesses, after which the linear root-finding procedure of the STD scheme is used. The VCP scheme is also included.

Scheme WSGR: This is the whole system groupwise rebalance scheme, described in Part IV, which is applied to the α eigenvalue search. Implementation is exactly as in the GCCMR scheme.

Scheme HYB: This is the hybrid scheme, also described in Part IV, in which both GCCMR and WSGR are performed for the α search, with both sets of rebalance factors being applied to the scalar flux and moments.

Scheme HYBNOF: This is the same as the above HYB scheme, except with no rebalance factors being applied to the fluxes. This scheme indicates how much of the acceleration is due to the improved α guess and how much acceleration is due to the rebalance factors themselves.

Scheme MXOUT5: This is identical to the HYB scheme, except that a maximum outer iteration limit of 5 outers for any one α guess is imposed, with one outer per α iteration for the first two α guesses, as described in Part V.

If all of the acceleration schemes provide a reduction in computational effort and have no interaction with the other methods, we would expect the last scheme, MXOUT5, to provide the greatest overall improvements.

Problem #1

This is a very small, hypothetical, one-group, two-material, spherical test problem. The material mesh and spatial mesh are shown in Fig. 1.

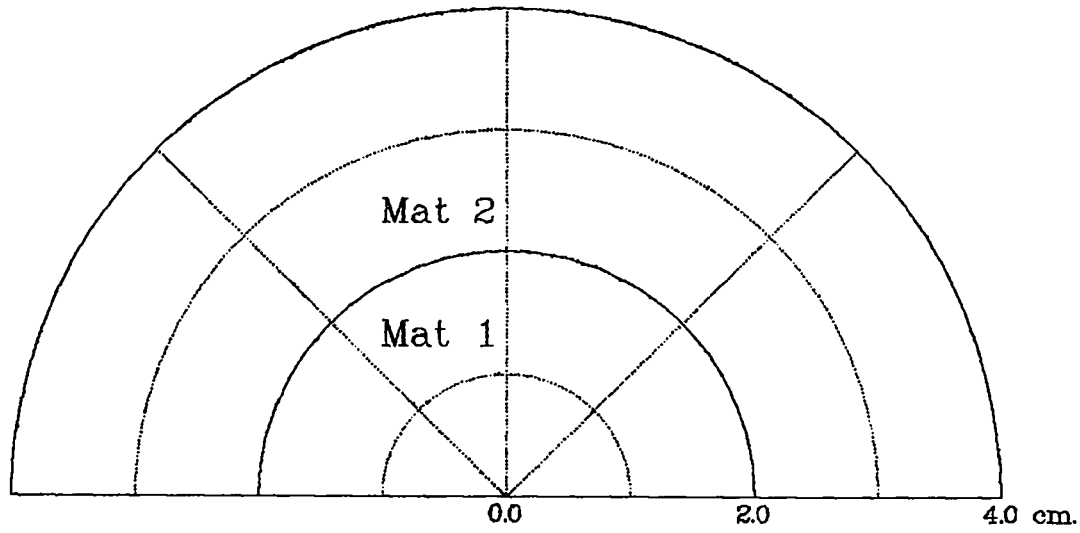

Fig. 1. Problem #1 material mesh and spatial mesh.

The macroscopic cross sections (cm^{-1}) for each material are

Mat	Σ_a	$\nu\Sigma_f$	Σ_t	$\Sigma_{1\to1}$
1	2.0	4.0	3.0	1.0
2	0.1	0	2.1	2.0

$\chi_1 = 1.0$ $\quad$ $v_1 = 10.0$ cm/sh

The results for this problem are

Scheme	Total Inners	
STD	678	
VCP	234	
GCCMR	157	(best rebalance)
WSGR	174	
HYB	157	
HYBNOF	157	(rebalance factors have no effect)
MXOUT5	123	

At the completion of the first α iteration (for which $k_{eff} = 1.835$), the two rebalance estimates of α are

Rebalance	α^1	
GCCMR	16.79	$\alpha_o = 18.32$
WSGR	8.42	

For the GCCMR at the end of the first α iteration, the complete eigenvalue spectrum and eigenvectors of rebalance factors are

	GCCMR Rebalance factors by material region
Eigenvalues	
$\alpha_0^1 = 16.79$	(1.738, 0.2615)
$\alpha_1^1 = -3.23$	(-0.1838, 2.1830)

At the completion of the third α iteration, the two GCCMR eigenvalues and eigenvectors are

Eigenvalues	Rebalance factors by material region
$\alpha_0^3 = 18.32$	(1.0004, 0.9996)
$\alpha_1^3 = -53.69$	(-0.0076, 2.0076)

From the above table of total inner iterations, we conclude

a. the variable convergence precision reduces the total inners by two-thirds.
b. the GCCMR is the more effective rebalance, which one would expect for a one-group problem.
c. no acceleration is coming from the rebalance factors.
d. the best overall improvement (MXOUT5 scheme) results in 1/5 the computational effort of the standard scheme.

Problem #2

This is another small, hypothetical, two-group, two-material, spherical test problem. The material and spatial meshes are the same as for Problem #1. The two group macroscopic cross sections (cm^{-1}) are

Mat	Group	Σ_a	$\nu\Sigma_f$	Σ_t	$\Sigma_{g\to g}$
1	1	2.0	4.0	3.0	1.0
	2	1.0	2.0	1.5	0.5
2	1	0.10	0	2.1	2.0
	2	0.20	0	4.2	4.0

$\Sigma_{1\to 2} = 0$ (no downscatter)

$\chi = (0.7, 0.3)$ $\quad v = (10.0, 0.1)$ cm/sh

The results for this problem are

Scheme	Total Inner	
STD	No convergence	
VCP	773	
GCCMR	714	
WSGR	531	(best rebalance)
HYB	534	
HYBNOF	557	(rebalance factors accelerate)
MXOUT5	266	

At the completion of the first α iteration (for which $k_{eff} = 1.816$), the two rebalance estimates of α are

Rebalance	α^1	
GCCMR	0.276	$\alpha_0 = 6.367$
WSGR	3.284	

For the GCCMR at the end of the first α iteration, the complete eigenvalue spectrum and eigenvectors of rebalance factors are

Eigenvalues	GCCMR Rebalance factors by material region
$\alpha_0^1 = 0.276$	(1.648, 0.3520)
$\alpha_1^1 = -0.105$	(-0.459, 2.459)

For the WSGR at the end of the first α iteration, the complete eigenvalue spectrum and eigenvectors of rebalance factors are

Eigenvalues	WSGR Rebalance factors by group
$\alpha_0^1 = 3.284$	(1.955, 0.0450)
$\alpha_1^1 = -0.150$	(5.267, -0.267)

From the above table of total inners, we conclude

a. the WSGR is the more effective rebalance, which one might expect because of the strong spectral skewing between the two material regions.

b. less than 5% of the acceleration is due to the rebalance factors.

c. the best overall improvement results from the MXOUT5 scheme, in one-third the computational effort of the worst case (VCP scheme).

Problem #3

This is a more realistic problem of a small central sphere (R = 5 cm) of H_2O, surrounded by a sphere of pure ^{235}U (R = 20 cm). All materials are at nominal density. A mesh spacing is used of 40 cells in the azimuthal direction and 20 cells in the radial direction (5 in the H_2O, 15 in the ^{235}U), as shown in Fig. 2.

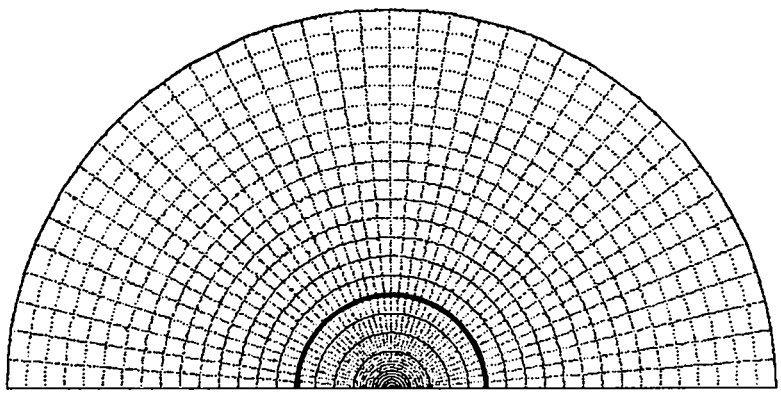

Fig. 2. Problem #3 material and spatial meshes.

A twelve-group, fast neutron cross-section set is used, with velocities ranging from v_1 = 51.93 cm/sh down to v_{12} = 0.00333 cm/sh.

The results for this problem are

Scheme	Total Inners	
STD	3511	
VCP	1175	
GCCMR	1147	
WSGR	984	(best rebalance)
HYB	983	
HYBNOF	1127	(rebalance factors accelerate)
MXOUT5	847	

At the completion of the first α iteration (for which k_{eff} = 1.706), the two rebalance estimates of α are

Rebalance	α^1	
GCCMR	0.479	α_0 = 0.844
WSGR	0.792	

For the GCCMR at the end of the first α iteration, the complete eigenvalue spectrum and eigenvectors of rebalance factors are

Eigenvalues	GCCMR Rebalance factors by material region
α_0^1 = 0.479	(1.9893 , 0.01071)
α_1^1 = -0.0028	(-0.1982 , 2.1982)

For the WSGR at the complete convergence of the problem, the eigenvalue spectrum for all 12 groups is shown in Fig. 3.

From the above table of total inners, we conclude

a. the variable convergence precision reduces the total inners by two-thirds.
b. the WSGR is the more effective, which one would expect from the strong spectral effect of the water.
c. about 15% of the acceleration is coming from the rebalance factors.
d. the best overall improvement (MXOUT5 scheme) results in 1/4 the computational effort of the standard scheme.

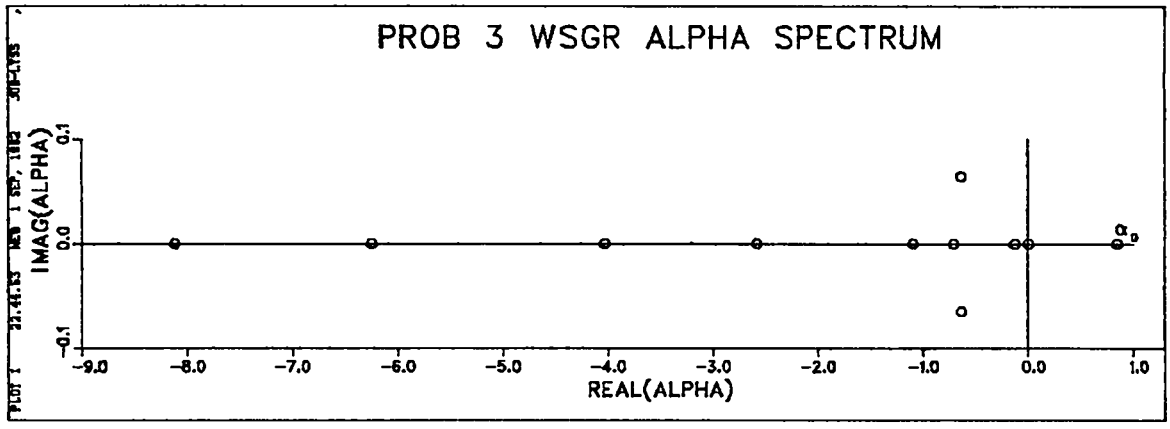

Fig. 3. Problem #3 WSGR α spectrum at convergence.

Problem #4

This is a five-material problem with a great deal of spatial inhomogeneity, consisting of concentric spheres of Al (R = 2 cm), ^{235}U (R = 16 cm), Fe (R = 17 cm), ^{238}U (R = 22 cm), and C (R = 26 cm), all at nominal density. The material and spatial mesh is shown in Fig. 4.

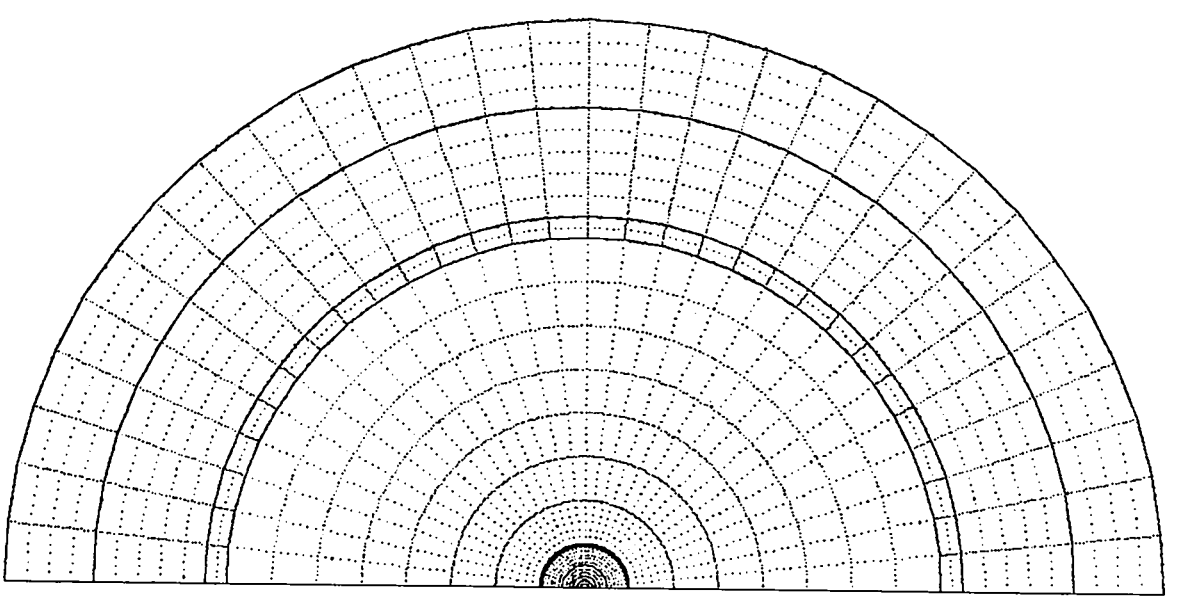

Fig. 4. Problem #4 material and spatial meshes.

The same 12-group cross-section set is used.

The result for this problem are

Scheme	Total Inners	
STD	5075	
VCP	1536	
GCCMR	1287	(best rebalance)
WSGR	1427	
HYB	1273	
HYBNOF	1315	(rebalance factors accelerate)
MXOUT5	1013	

At the completion of the first α iteration (for which $k_{eff} = 1.726$), the two rebalance estimates of α are

Rebalance	α^1	
GCCMR	0.620	$\alpha_0 = 0.826$
WSGR	0.538	

For the GCCMR at the end of the first α iteration, the complete eigenvalue spectrum and eigenvectors of rebalance factors are

Eigenvalues	GCCMR Rebalance factors by material region				
$\alpha_0^1 = 0.620$	(1.427	1.652	1.142	0.529	0.247)
$\alpha_1^1 = -0.258$	(0.119	0.112	-0.419	-1.50	-2.85)
$\alpha_2^1 = -0.803$	(-0.092	-0.074	0.480	1.41	-2.94)
$\alpha_3^1 = -3.97$	(-4.93	0.012	0.046	-0.008	0.001)
$\alpha_4^1 = -4.82$	(0.638	-0.138	3.64	-0.515	-0.005)

For the WSGR at the complete convergence of the problem, the eigenvalue spectrum for all 12 groups is shown in Fig. 5.

The rebalance factors at the end of the first α iterations are those factors required to convert the k_{eff} solution fluxes to the converged α solution fluxes. By performing a k_{eff} ($\alpha = 0$) calculation, then performing the full α calculation, and then integrating both sets of fluxes over all groups and each coarse mesh zone, it is possible to calculate the exact rebalance factors that are required to convert the k_{eff} solution to the converged α solution. These exact rebalance factors are compared to the approximate rebalance factors at the end of the first α iteration below.

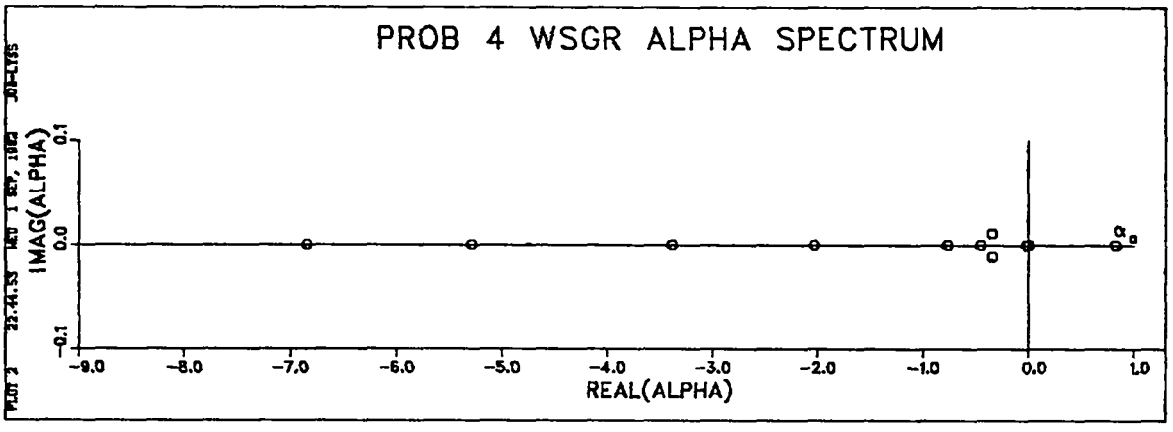

Fig. 5. Problem #4 WSGR α spectrum at convergence.

Rebalance factors by material zone

Exact	GCCMR
1.581	1.429
1.481	1.653
0.911	1.142
0.634	0.529
0.394	0.247

Rebalance factors by group

Exact	WSGR
2.519	2.265
2.438	2.220
2.272	2.121
1.999	1.936
1.377	1.470
0.723	0.904
0.375	0.549
0.187	0.326
0.108	0.199
3.37 E-4	1.16 E-2
2.39 E-6	1.19 E-4
9.84 E-10	1.56 E-5

From the above tables, we conclude

a. the variable convergence precision reduces the total inners required by 2/3.

b. the GCCMR is more effective, which one might expect from the considerable spatial structure of this problem.

c. only about 3% of the acceleration is coming from the rebalance factors.

d. the best overall improvement (MXOUT5 scheme) results in 1/5 the computational effort of the standard scheme.

Problem #5

This is a simple, homogeneous, three-group, spherical test problem with a radius of 4.0 cm. The problem was run as a 90° segment of the sphere, using 64 mesh cells in the azimuthal direction and 64 mesh cells in the radial direction as shown in Fig. 6.

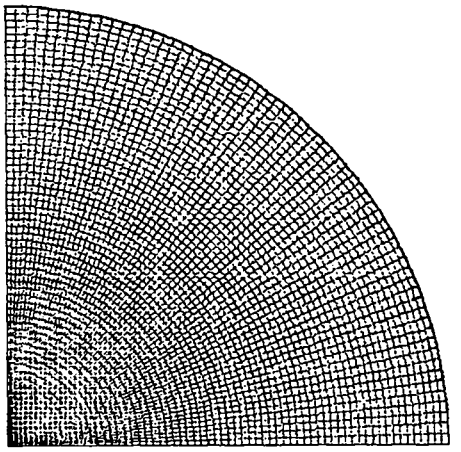

Fig. 6. Problem #5 fine spatial mesh (64 x 64).

The hypothetical three-group macroscopic cross sections, representing two fast groups and a thermal group are

Group	Σ_a	$\nu\Sigma_f$	Σ_t	$\Sigma_{g\to g}$	$\Sigma_{g-1\to g}$	$\Sigma_{g-2\to g}$
1	0.25	0.75	0.80	0.25	--	--
2	0.20	0.60	0.70	0.30	0.20	--
3	0.10	0.30	10.0	9.90	0.20	0.10

χ = (0.75, 0.2, 0.05)

v = (10.0, 0.1, 0.001) cm/sh

One of the defects of coarse mesh rebalance is its instability as the rebalance mesh approaches the fine mesh, for some problems. This problem is designed to see if that defect occurs for the α CMR equations. The spatial rebalance mesh is obtained by repeatedly dividing the spatial domain in both the radial and azimuthal directions. Thus, the problem is run with 1 (4096 cells/coarse mesh zone: mesh A), 4 (1024 cells/coarse mesh zone: Mesh B), 16 (256 cells/coarse mesh zone: Mesh C), and 64 (64 cells/coarse mesh zone: Mesh D) coarse mesh rebalance zones. In addition, the problem is run with a coarse 8 x 8 spatial mesh and 64 (1 cell/coarse mesh zone: Mesh DCM) rebalance zones; thus, fine mesh rebalance.

The results for this problem are

Scheme	Total Inners A	B	C	D	DCM[a]
STD	1196	729	452	374	b
VCP	218	201	178	137	b
GCCMR	285	244	222	170	b
WSGR	225	110	83	52	b
HYB	225	110	95	61	b
HYBNOF	233	141	97	64	b
MXOUT5	162	111	78	71	114

[a] Fine mesh rebalance: 8 x 8 coarse spatial mesh.
[b] First set of outer iterations fails to converge.

At the completion of the first α iteration (for which $k_{eff} = 1.948$), the two rebalance estimates of α for each mesh are

Rebalance	A	B	C	D	DCM[a]
GCCMR	0.00041	0.00041	0.00041	0.00040	0.00040
WSGR	0.425	0.456	0.475	0.476	0.382
		$\alpha_0 = 0.485$			$\alpha_0 = 0.491$

For the fine mesh rebalance case (Mesh DCM), the first set of outer iterations fails to converge, falling into a two-cycle oscillating mode, which prevents the convergence of λ, except for the MXOUT5 scheme in which the outer iteration limit terminates the outers. With the outer iteration limit imposed, both α rebalance schemes, GCCMR and WSGR, perform well and give no indication of a stability problem for fine mesh rebalance. The GCCMR gives particularly poor estimates of α for this problem. This might be expected, since the spatial distribution for the k_{eff} problem and the α problem do not differ greatly for homogeneous systems.

For the GCCMR at the complete convergence of the problem, the eigenvalue spectra for the various rebalance meshes are shown in Fig. 7.

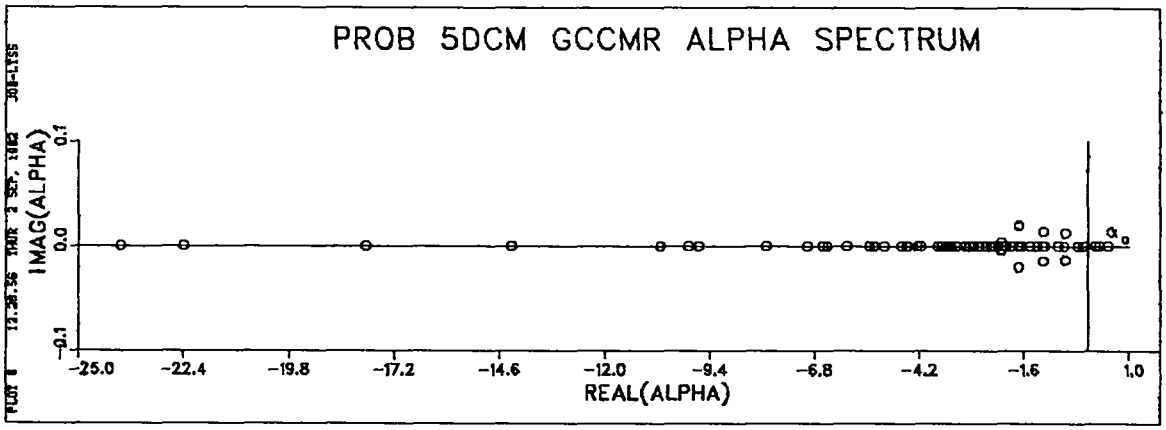

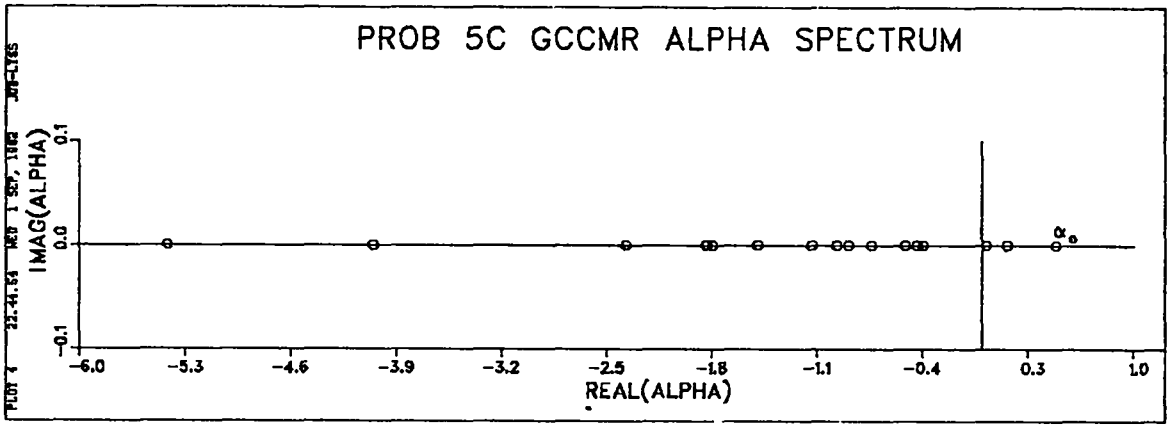

Fig. 7. Problem #5 GCCMR α spectra at convergence.

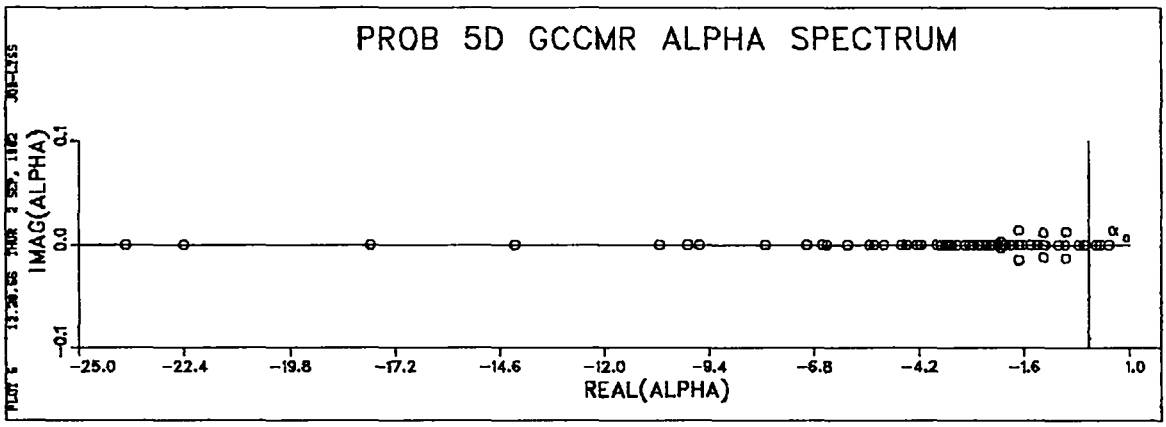

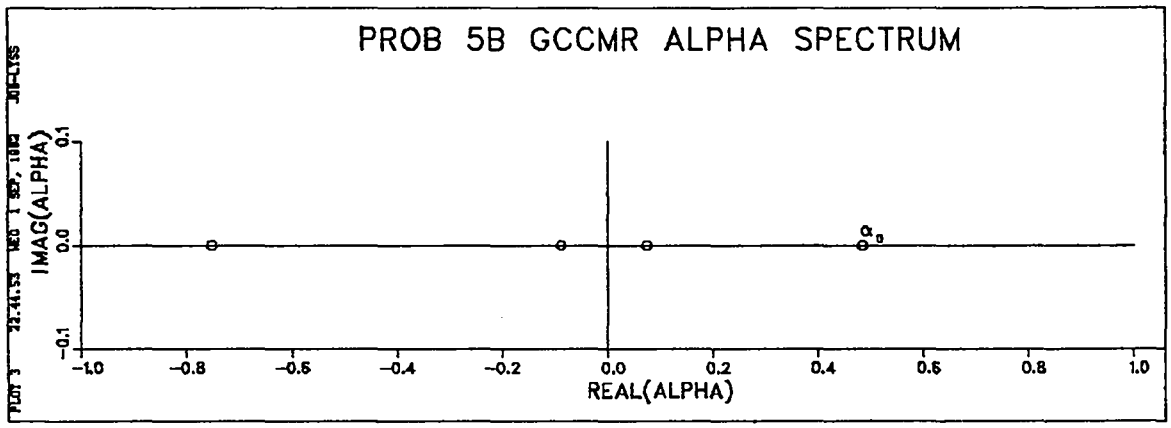

Fig. 7. Continued.

For this problem, we conclude

a. the variable convergence precision reduces the total inners required by 4/5 to nearly 2/3.
b. the WSGR is more effective, which one might expect from the strong spectral effect due to the bottom group.
c. neither the GCCMR or WSGR appears to have stability problems when the rebalance mesh and fine mesh are identical.
d. only a few per cent of the acceleration is coming from the rebalance factors.
e. the best overall improvement (MXOUT5) scheme results in 1/8 to 1/5 the computational effort of the standard scheme.

VII. SUBCRITICAL SEARCHES

Alpha eigenvalue searches for subcritical systems are notoriously difficult to converge. For highly subcritical systems, a code crash (referred to as a "dramatic failure" in the code manuals[1-3]) is the usual result. In this section, we examine the causes for the code "failure" and describe a remedy for this deficiency.

There are many elegant mathematical papers[6-10] written on the α eigenvalue spectrum of Eq. (3). These can be summarized, for the most interesting case of a finite media, as follows:[9] For the continuous velocity variable, $v \in [0,\infty)$, including the limit $v = 0$, there exists a continuum of eigenvalues to the left of α^*, where

$$\alpha^* = - \max_{\vec{r}} \lim_{v \to 0} v\Sigma_t(v) \quad , \tag{24}$$

and there may exist a discrete spectrum of points and, possibly, curves to the right of α^*, as illustrated in Fig. 8. The existence of a discrete-eigenvalue spectrum is not guaranteed. If a discrete-eigenvalue spectrum exists, it has been shown[18,19] there exists a dominant eigenvalue, α_0, with $\text{Im}\ \alpha_0 = 0$, $\alpha_0 > \alpha^*$, and $\psi_\alpha > 0$.

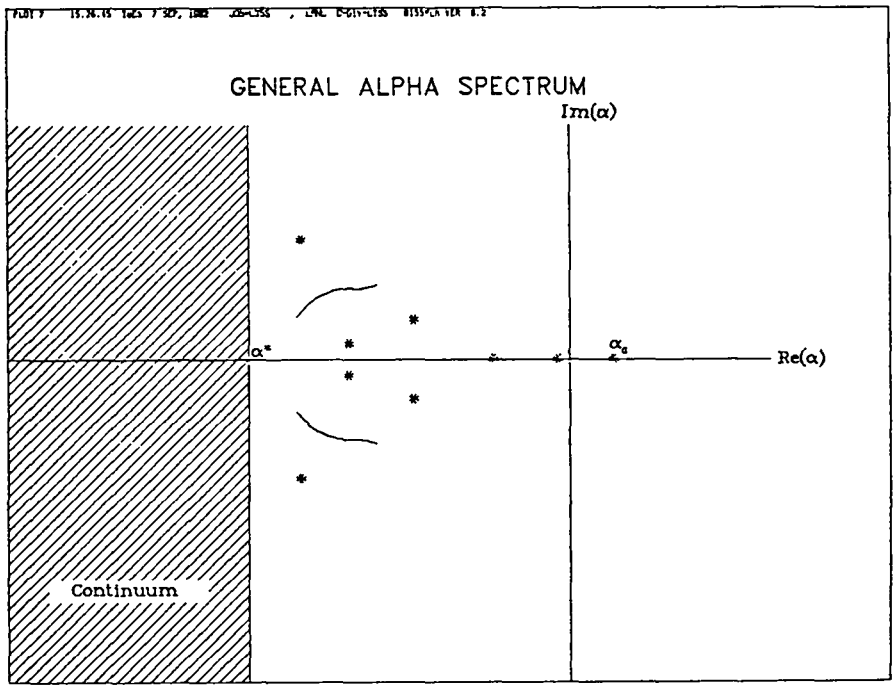

Fig. 8. General eigenvalue spectrum.

For velocity space bounded away from zero, $v \in (v_0,\infty)$, $v_0 > 0$, the continuum spectrum in Fig. 8 becomes a discrete spectrum of points and, possibly, curves.

In the former case in which $v_0 \geq 0$, for sufficiently small bodies, the point spectrum to the right of α^* in Fig. 8 can disappear. In this situation, the time-dependent flux decay is dominated by the $v \to 0$ limit, by neutrons that are moving very slowly through the medium. There has been considerable mathematical discussion on this "disappearance of the point spectrum into the continuum" and the existence of point eigenvalues within the continuum. Larsen and Zweifel[9] argue that this continuum part of the spectrum is a creature of the mathematics and does not correspond to physical reality; that at velocities $v \to 0$, quantuum mechanical effects probably render the transport equation invalid. At these very low velocities, the neutron population density is undoubtedly so low as to make the transport equation inapplicable.

The case of the transport equation in the multigroup approximation has been analyzed by Larsen[10] and these esoteric mathematical ambiguities do not exist.

Under simple conditions on the cross sections that are virtually always met in practice (namely, that a neutron or its progeny in any one group can eventually transfer to any other group), he proved the existence of a dominant eigenvalue α_0 and a corresponding positive eigenfunction ψ_α . Thus, the failure of transport codes (which solve the multigroup transport equation) to calculate an α eigenvalue for a subcritical system is <u>not</u> due to the eigenvalue's nonexistence but due to some deficiency in the computational procedure.

For supercritical systems, α_0 (>0) corresponds to a physically measurable quantity, the exponential growth of the flux at long times after any early transients (with $\alpha_i < 0$) have died out. The possibility of driving a nuclear system sufficiently supercritical to be supercritical in a higher eigenmode apparently has not been examined.

For subcritical systems ($\alpha_0 < 0$), the physical interpretation of the dominant eigenvalue α_0 has been subject to some debate. There are some strong arguments* that <u>no</u> valid physical interpretation of the negative dominant eigenvalue (guaranteed by the multigroup transport equation) can be made, no matter how close to critical is the system. For some physical systems, experimenters have actually been unable to measure <u>any</u> pulsed neutron experiment die-away constants.[8,†] However, exponential die-away constants for subcritical GODIVA assemblies[17,†] for water assemblies,[8] and for natural uranium systems[13] and Rossi-α[17] constants for various systems[17] have been measured and, in some cases,[13] have been found in good agreement with calculations.

For highly absorbing and for subcritical systems, the long-time or asymptotic distribution is dominated by very slowly moving neutrons. In this regime, the multigroup assumption may be a very poor approximation. The neutron population densities may be so low and neutron wave and other quantum effects so large that the results from a multigroup transport calculation have little relation to physical reality. Thus, <u>code users should exercise considerable caution in physical interpretations of the calculated α_0 for far subcritical systems</u>. This is demonstrated in the example problem to follow.

---

*P. P. Whalen, Los Alamos National Laboratory Group X-DO, provided this information (1982).

†G. E. Hansen, Los Alamos National Laboratory, Group Q-2, provided this information (1982).

We will assume that the code user, for whatever reason, has a genuine need to calculate an α eigenvalue for a subcritical system. It is then necessary to understand why the present eigenvalue search algorithm fails, in order to devise a remedy.

If, at some point during the search, the α eigenvalue guess becomes sufficently large and negative, then the effective total cross section,

$$\Sigma_{t,eff} = \Sigma_{t,g} + \frac{\alpha}{v_g} \quad ,$$

may become negative for some energy groups and mesh cells. Such negative total cross sections obviously have no meaning for the transport equation and the solution algorithms will assuredly fail. Thus, if one constrains the α search procedure to maintain

$$\alpha \geq \alpha^* = - \max_{ij} \min_{g} v_g \Sigma_{t,g} \quad , \tag{25}$$

which will usually occur in the bottom energy group (g = IGM), then negative effective total cross sections will not occur.

Unfortunately, this constraint is insufficient to insure convergence of the α eigenvalue search algorithm. Convergence failure will also occur when an α guess becomes sufficiently small so that the system becomes <u>supercritical</u> in one of the groups. Neglecting leakage, this will occur when

$$\Sigma_{t,g} + \frac{\alpha}{v_g} < \Sigma_{s,g} \tag{26}$$

for some energy group g. When α becomes sufficiently large and negative so that, with leakage, some group becomes supercritical, the inner iterations will fail to converge for that group and, with subsequent additional outer or inner iterations, the flux will diverge until machine overflow occurs, the so-called "dramatic code failure."

To illustrate this situation, consider a homogeneous uranium sphere of radius 8.74 cm, composed of 75% ^{238}U and 25% ^{235}U, at normal density. For a five-group cross-section set and an S_2P_0 approximation, a plot of λ versus α is shown in Fig. 9.

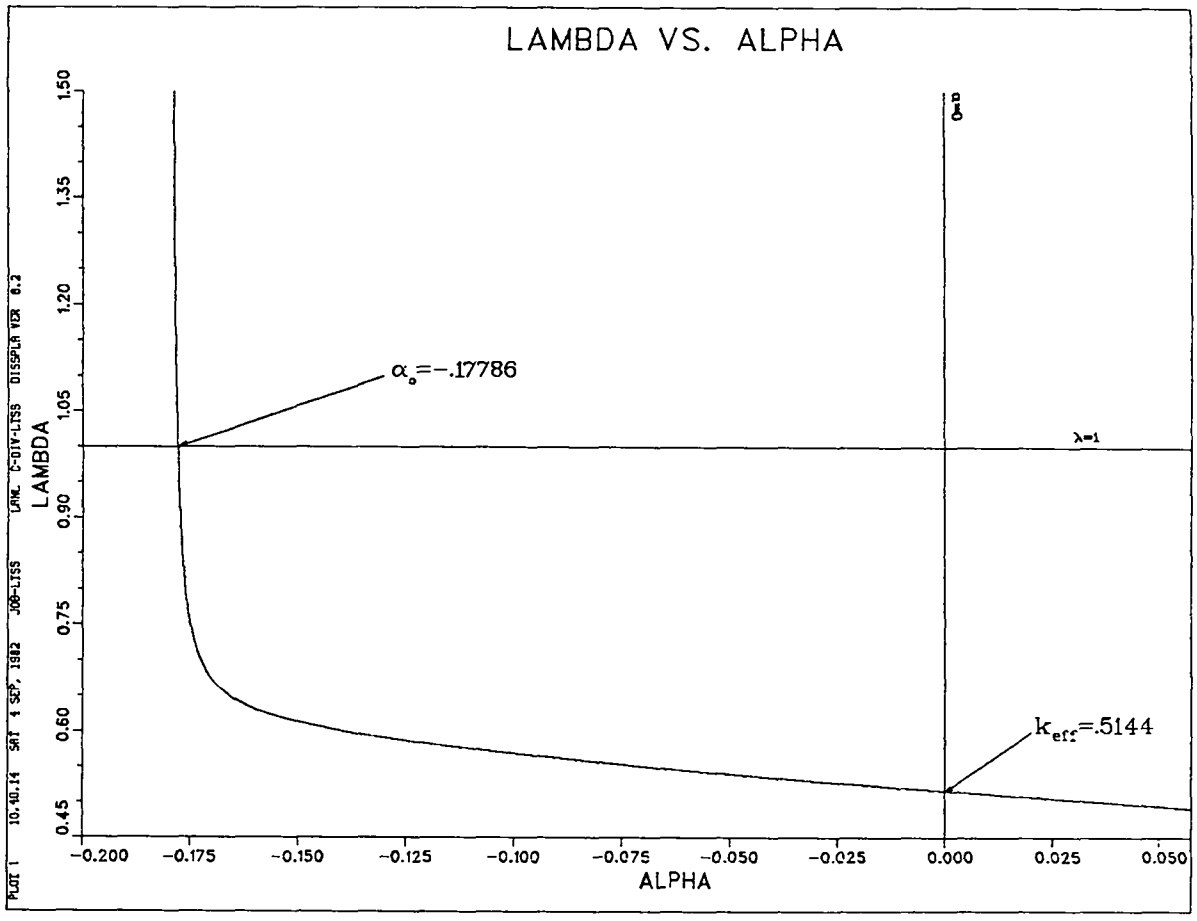

Fig. 9. $\lambda(\alpha)$ for subcritical uranium sphere.

For this problem, the system becomes supercritical in the bottom group whenever α < - 0.18 generations/shake (1 shake = 10^{-8} s).

From this curve in Fig. 9, it is obvious why a conventional α eigenvalue search technique will fail. The linear extrapolation from the first two $\lambda(\alpha)$ points will yield a guess of α << - 0.18 gen/sh, far into the region of iteration divergence ($\alpha < \alpha_{min}$). This is illustrated in Fig. 10.

It should be pointed out that $\alpha^* = -1.018$ gen/sh for this cross-section set, so that the region of iteration divergence ($\alpha < \alpha_{min}$) is bounded well to the right of the theoretical minimum.

The solution to the failure of α eigenvalue searches for subcritical systems is straightforward. We wish to

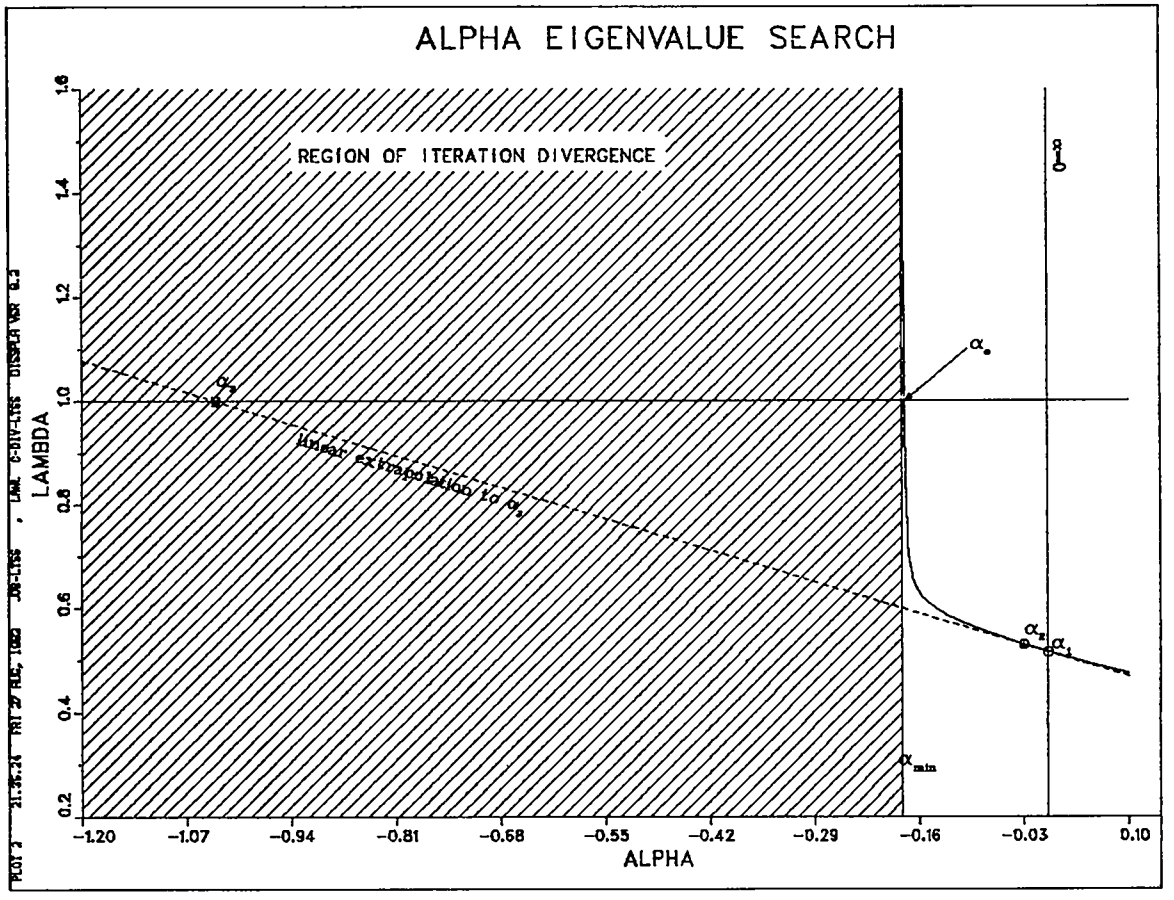

Fig. 10. Failure of α search procedure.

1. attempt to determine α_{min} so that any extrapolation will not enter the region of iteration divergence, and
2. restart the α search whenever it extrapolates into this region of iteration divergence.

The modifications to the search procedure are relatively minor:

- Set the inner iteration limit to a moderately large number (say 50).
- Monitor the inner iterations for divergence.
  1. If the inner iteration limit is reached in any group, then the current α^n (n = α iteration index) is too far negative. Abort the current outer iteration. Store the current α^n into α_{min} if α^n > current α_{min}.

2. Choose a new α^{n+1} midway between this current α^{n} (for which the inners diverged) and the last α^{n-1} for which the outers converged

$$\alpha^{n+1} = (\alpha^{n} + \alpha^{n-1})/2$$

3. Start a new set of outer iterations.

- Constrain the α guesses so that $\alpha^{n+1} > \alpha_{min}$.

1. If the linear or quadratic extrapolation or the rebalance procedure gives an $\alpha^{n+1} < \alpha_{min}$, then choose the next $\alpha^{n+1} = \alpha_{min} + \delta_{n}$, where δ is some small arbitrary number that changes with α iteration index n (say $\delta = 0.01/n$).

The success of this procedure is illustrated for the subcritical uranium sphere in Fig. 11, where the λ's for the various α guesses are plotted. In this case, the GCCMR scheme was utilized for the first two α iterations (namely α^{2} and α^{5}), rather than an eigenvalue modifier and a linear extrapolation. Once an α^{n} for which $\lambda > 1$ is found, the eigenvalue iterations converge very rapidly.

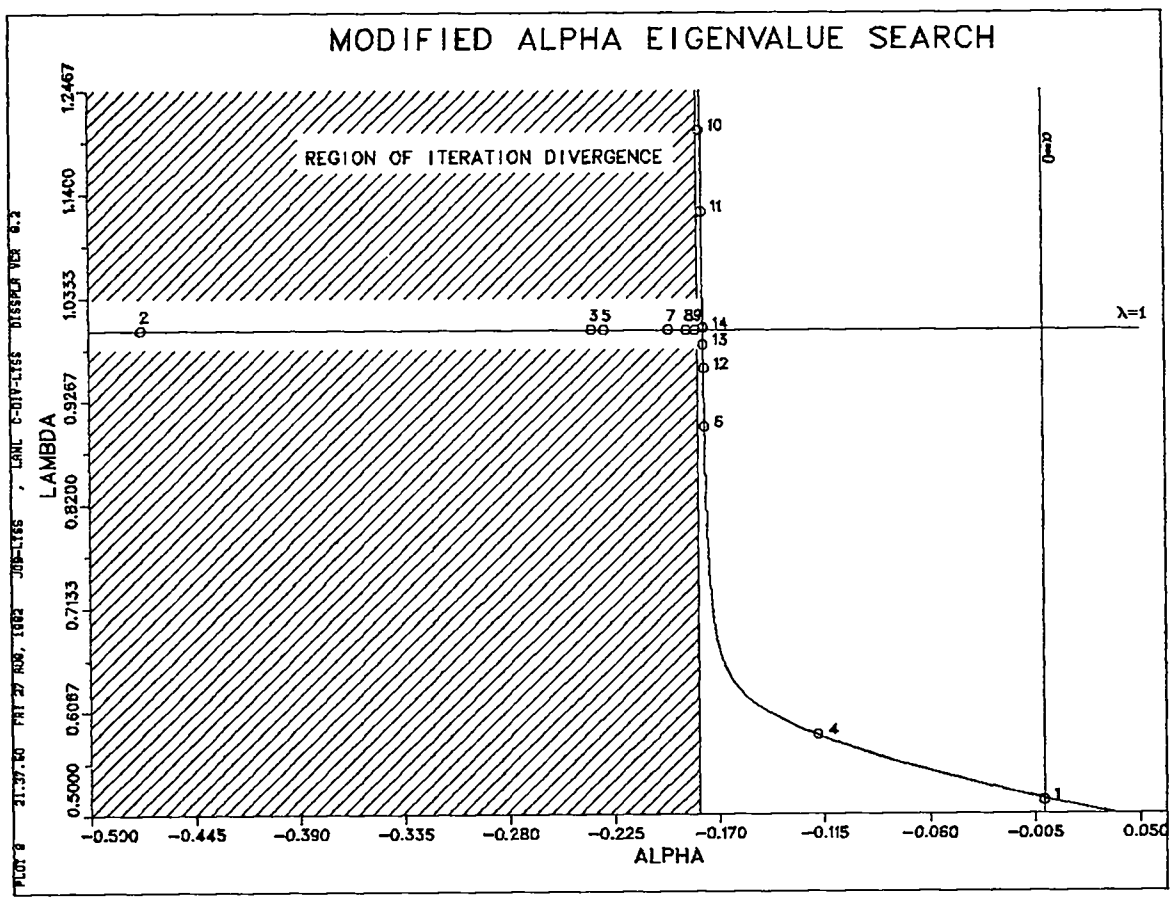

Fig. 11. Modified search procedure.

It should be noted that all current discrete-ordinates transport codes cannot calculate α eigenvalues for systems without any fissile material, since the λ eigenvalue is not defined for such systems. To modify these codes whose eigenvalue search procedure is based on roots of the $\lambda(\alpha)$ curve requires rather major surgery to the code. However, a code whose eigenvalue search is based entirely on a rebalance scheme, which does not require the λ eigenvalue, can be modified with little effort to calculate such eigenvalues.

The α search procedure described above is sufficiently robust to yield the dominant eigenvalue of the multigroup transport equation, $\alpha_0 = -0.178$, for this problem and this multigroup structure. One might ask if this computed α_0 is a physically meaningful quantity; if this α_0 corresponds to an exponential die-away constant for this system. In this case, the answer is probably no.

By changing the cross-section multigroup structure, one finds that the α_0 for this problem is extremely sensitive to changes in the bottom energy group. By changing the lowest group velocity by a factor of 2 (v_5 = 1.444 cm/sh → 2.888 cm/sh), then α_0 = -0.178 gen/sh → -0.351 gen/sh, or also changes by a factor of 2, with no change in k_{eff}. Conversely, if one increases the group 1 $\nu\Sigma_f$ by a factor of 2, one noticeably increases k_{eff}, but there is virtually no change in α_0. Thus, for this problem, the calculated α_0 is virtually a function only of the multigroup structure and, in particular, the bottom neutron energy group speed. In this case, it is highly suspect that the calculated α_0 has any meaningful relation to physical reality.

One can continue to increase the $\nu\Sigma_f$ in the cross sections until the point is reached that the α_0 is sensitive to these changes in the cross section. Once this point is reached, one finds that the computed α_0 is now relatively insensitive to changes in the bottom energy group. For example, if the group 3 $\nu\Sigma_f$ is multiplied by 2.5, the system is only slightly subcritical (k_{eff} = 0.940). By changing the lowest group velocity by a factor of 2 (v_5 = 1.444 cm/sh → 2.888 cm/sh), then α_0 = -0.087 gen/sh → -0.090 gen/sh, or α_0 only changes by 3%.

This behavior of the eigenvalues for this problem leads to the following conjecture. The $\lambda(\alpha)$ curve, as shown in Fig. 9, may be, perhaps, the superposition of two separate curves, as shown in Fig. 12. Curve 1 and its eigenvalue α_1 may be associated with some composite properties of the system, while curve 2 and its eigenvalue α_2 (= α_0, the dominant eigenvalue, in this case) are associated with the behavior of the most slowly moving neutrons in the bottom energy group. In this situation, the calculated dominant eigenvalue, α_0, has no relation to a physically measurable die-away constant.

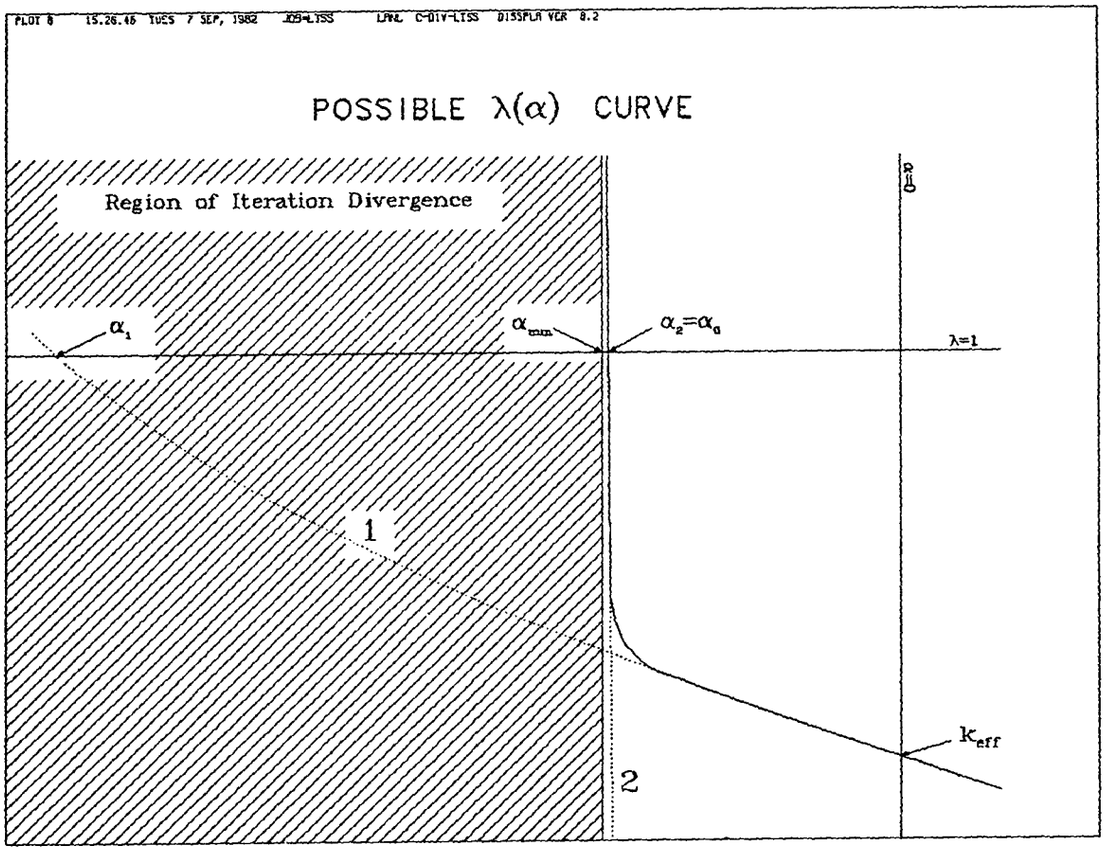

Fig. 12. Possile λ(α) curve.

As the system is driven towards criticality, curve 1 is moved upward until eventually its associated eigenvalue, α_1, becomes the dominant eigenvalue, α_0, a quantity insensitive to the behavior of the neutrons in the bottom group. At this point, the dominant eigenvalue of the multigroup transport may correspond to a physical die-away constant. Whether the curve 1 eigenvalue, α_1, as originally shown in Fig. 12, corresponds to a "discrete eigenvalue buried in the continuum," one can only guess.

One can summarize the discussion in this section of subcritical α eigenvalues as follows:

- A robust eigenvalue search procedure has been developed to obtain the dominant eigenvalue of the multigroup transport equation, a quantity whose existence is guaranteed under the most general conditions.

The code user must be extremely careful in his interpretation of this dominant eigenvalue as a physically meaningful exponential die-away constant. If his computed eigenvalue is sensitive to the bottom energy group velocity, it is highly suspect. That is to say, if his system is sufficiently subcritical so that the improved search procedure is invoked by the code, the computed dominant eigenvalue most likely has little relation to physical reality. Stated another way, a "dramatic code failure" is nature's way of saying the user is calculating nonsense.

VIII. CONCLUSIONS

The two rebalance schemes are found to accelerate the α eigenvalue calculation by anywhere from a small amount to as much as 50% and more, as compared with the variable convergence precision scheme. Nearly all of the acceleration comes from the improved estimates of α, with very little, in most cases, coming from the rebalance factors themselves.

More importantly, the rebalance scheme makes the iterative solution of the α eigenvalue problem considerably more robust, relieves the code user of much of the burden of providing intelligent input required by the standard search procedure, and permits modifications to the iteration strategy that eliminates many of the unnecessary calculations. By utilizing all the schemes and procedures described in this report, we can usually solve the α eigenvalue problem in one-fifth the time required for the present search procedure.

ACKNOWLEDGEMENT

Credit is given to Warren F. Miller, Jr. for observing the applicability of coarse mesh rebalance to the α eigenvalue problem and many subsequent discussions. Appreciation is expressed to Edward W. Larsen for his truly enlightening discussions and clarification of much of the esoteric mathematical literature. Much of this report has evolved over the last several years from cooperative efforts with a number of X-Division personnel. Acknowledgement is made particularly to Paul P. Whalen for his contributions.

APPENDIX

IMPLEMENTATION OF α REBALANCE ACCELERATION

The two α rebalance schemes (GCCMR and WSGR) were implemented and tested in the Lagrangian mesh discrete-ordinates code LaMEDOC[14]. In this appendix, we will give the coding details for their implementation in LaMEDOC. We will first describe the important variable names. The actual code listing will then be given, broken down into numbered segments. Finally, the purpose of each numbered segment of coding will be described.

The SUBROUTINE AREBAL (ALFAN), the mnemonic for α rebalance, provides the new α guess (ALFAN), using the fluxes stored in common at the completion of the current set of outer iterations.

The important integer variables are

NMAT: number of materials in the problem. The coarse mesh rebalance is performed on the material mesh, so that NMAT is actually the number of coarse mesh regions.

IGM: number of energy group (= IGMD).

LM,KM: number of mesh cells in the two dimensions of the Lagrangian mesh.

The important arrays are

FLUX(NM,KMLM,IGM): the scalar flux and moments (NM moments total) for each of the KMLM (= KM*LM) Lagrangian mesh cells and for each of IGM energy groups.

FLGS(k,ℓ): the group-summed negative inflows from material zone k to material zone ℓ, with FLGS (k,k) being the total outflow from material zone k. This is the matrix of Eq. (11), used in the GCCMR.

F(k): the GCCMR rebalance factors, for NMAT material zones.

NL(g): the groupwise net leakage from the system, used in the WSGR.

FSS(k): the volume-integrated fission source for the k'th material mesh zone. This is Eq. (9b), used in the GCCMR.

ABSP(k): the volume-integrated absorption for the k'th material mesh zone. This is Eq. (9a), used in the GCCMR.

FV(k): the total neutrons for the k'th material mesh zone. This is Eq. (9c), used in the GCCMR.

RA(k,ℓ): the FL+AB-FS array on the left-hand side of Eq. (8) of the GCCMR.

Q(k): the FV*f vector on the right-hand side of Eq. (8) of the GCCMR.

WSRC(g): the C_g diagonal matrix of Eq. (21b) for the WSGR.

WSRFV(g): the FV_g diagonal matrix of Eq. (21c) for the WSGR.

WSRS(g,g'): the $S_{gg'}$ array of Eq. (21d) for the WSGR.

WSRFS(g,g'): the $FS_{gg'}$ array of Eq. (21e) for the WSGR.

WSFSS(g): the whole system fission source for each group g. Used in the WSGR to maintain the total fission source normalization of unity.

WSF(g): the rebalance factors for group g of the WSGR.

WSRA(g,g'): the NL+C-S-FS array on the left-hand side of Eq. (20), for the WSGR.

WSQ(g): the FV*f vector on the right-hand side of Eq. (20), for the WSGR.

The following two pages contain the listing of the AREBAL routine.

```
      SUBROUTINE AREBAL(ALFAN)
C
C     PERFORM MATERIAL MESH REBALANCE ACCELERATION OF ALFA
C
      OPTIMIZE
      MACRO PARAMC (CLCHFILE)  $  USE PARAMC (CLCHFILE)
      MACRO CONSTC (CLCHFILE)  $  USE CONSTC (CLCHFILE)
      MACRO FLUXSC (CLCHFILE)  $  USE FLUXSC (CLCHFILE)
      MACRO XSECC (CLCHFILE)   $  USE XSECC (CLCHFILE)
      MACRO SETLC (CLCHFILE)   $  USE SETLC (CLCHFILE)
      MACRO MESHC (CLCHFILE)   $  USE MESHC (CLCHFILE)
      DIMENSION WSRC(IGMD),WSRS(IGMD,IGMD),WSRFS(IGMD,IGMD),WSRFV(IGMD),
     1          WSRA(IGMD,IGMD),WSQ(IGMD),WSF(IGMD),WSFSS(IGMD)
      EQUIVALENCE (WSF(1),WSQ(1))
      INTEGER GP
      INTEGER G                                                          Code
      DIMENSION VELI(IGMD)                                               Block
      COMMON/CONVG/ EPSL,EPSO,EPSI
C
C
C     SCALE FLOWS BY LAST OUTER REBALANCE (OREBAL) FACTOR
      DO 18 L=1,NMAT  $  DO 18 K=1,NMAT
   18 FLGS(K,L)=F(K)*FLGS(K,L)                                              1
C     LAST OUTER REBAL FACTOR = 1/ALA , SCALE NET LEAKGE
      DO 19 G=1,IGM
   19 NL(G)=NL(G)/ALA
C     CALCULATE FISSION SOURCE ON MATERIAL MESH
      CALL CLEAR(0.0,FSS,NMAT)
      DO 20 L=1,LM $ DO 20 K=1,KM  $  MAT=IM(K,L)+1                         2
   20 FSS(MAT)=FSS(MAT)+FISSA(K,L)*VOL(K,L)
C     CALCULATE ABSORPTION (SANS ALFA/VEL) AND FV ON MATERIAL MESH
      CALL CLEAR(0.0,ABSP,NMAT)  $  CALL CLEAR(0.0,FV,NMAT)
      DO 25 G=1,IGM
   25 VELI(G)=1./VEL(G)
      DO 30 L=1,LM $ DO 30 K=1,KM  $  KL=(L-1)*KM+K  $  MAT=IM(K,L)+1       3
      DO 28 IPOS=1,18  $  IF(FR(IPOS,K,L)) ,28
      IX=MATIX(IPOS,MAT)  $  ATOMS=ANO(K,L)*FR(IPOS,K,L)
      DO 27 G=1,IGM
   27 ABSP(MAT)=ABSP(MAT)+ATOMS*SIGA(G,IX)*FLUX(1,KL,G)
   28 CONTINUE
      DO 30 G=1,IGM
   30 FV(MAT)=FV(MAT)+VELI(G)*FLUX(1,KL,G)*VOL(K,L)
C
      IF(NMAT.EQ.1) THEN
C        ONE MATERIAL, DO NOT ITERATE                                      4
         XLA=(FSS(1)-FLGS(1,1)-ABSP(1))/FV(1)  $  F(1)=1.0
         GO TO 155
         END IF
C     BEGIN INVERSE POWER ITERATION FOR ALFA EIGENVALUE
      XLA=10.0  $  T=0.0
      DO 90 K=1,NMAT
   90 T=T+FSS(K)  $  CALL CLEAR(T,F,NMAT)
C
  100 CONTINUE
      DO 104 L=1,NMAT  $  DO 102 K=1,NMAT                                   5
  102 RA(K,L)=FLGS(K,L)
      Q(L)=FV(L)*F(L)
  104 RA(L,L)=RA(L,L)+ABSP(L)-FSS(L)+XLA*FV(L)
      CALL LSS(NMAT,1,NMAT,RA,Q ,DUMY,DET)
      TP=T  $  T=0.0
      DO 110 L=1,NMAT
  110 T=T+FSS(L)*F(L)
      TA=1./T  $  XLAR=XLA  $  XLA=XLAR-TA
      DO 112 L=1,NMAT
  112 F(L)=TA*F(L)
      IF(ABS(1.-XLA/XLAR).GT.EPSO) GO TO 100
C
C     DO WHOLE-SYSTEM GROUP-WISE REBALANCE
C     GENERATE WSR MATRICES                                              6
  155 CALL CLEAR(0.0,WSRC,IGM) $ CALL CLEAR(0.0,WSRS,IGM*IGM)
      CALL CLEAR(0.0,WSRFV,IGM) $ CALL CLEAR(0.0,WSRFS,IGM*IGM)
      DO 200 L=1,LM $ DO 200 K=1,KM $ KL=(L-1)*KM+K $ MAT=IM(K,L)+1
      DO 180 IPOS=1,18  $  IF(FR(IPOS,K,L)) ,180
      IX=MATIX(IPOS,MAT)  $  ATOMS=ANO(K,L)*FR(IPOS,K,L)
      DO 160 G=1,IGM                                                     7
      WSRC(G)=WSRC(G)+ATOMS*SIGTOT(G,IX)*FLUX(1,KL,G)
      WSRFS(1,G)=WSRFS(1,G)+ATOMS*SIGNU(G,IX)*FLUX(1,KL,G)
      DO 160 GP=1,G  $  INDXG=(G*(G-1))/2+GP
  160 WSRS(G,GP)=WSRS(G,GP)+ATOMS*SIGDS(1,INDXG,IX)*FLUX(1,KL,GP)
  180 CONTINUE
```

```
      DO 182 G=1,IGM
  182 WSRFV(G)=WSRFV(G)+FLUX(1,KL,G)*VOL(K,L)*VELI(G)
  200 CONTINUE
C     SAVE GROUP-WISE WS FISSION SOURCE FOR NORMALS
      DO 220 G=1,IGM
  220 WSFSS(G)=WSRFS(1,G)
C     FILL OUT FISSION MATRIX                                          8
      DO 210 G=2,IGM  $  DO 210 GP=1,IGM
  210 WSRFS(G,GP)=WSRFS(1,GP)
      DO 212 G=1,IGM  $  DO 212 GP=1,IGM
  212 WSRFS(G,GP)=CHI(G)*WSRFS(G,GP)
      XXLA=10.0  $  T=0.0
      DO 290 G=1,IGM
  290 T=T+WSFSS(G)  $  CALL CLEAR(T,WSF,IGM)
C
C     START INVERSE POWER ITERATION
  300 CONTINUE
      DO 320 G=1,IGM  $  DO 320 GP=1,IGM
  320 WSRA(G,GP)=-WSRS(G,GP)-WSRFS(G,GP)
      DO 322 G=1,IGM  $  WSQ(G)=WSF(G)*WSRFV(G)                        9
  322 WSRA(G,G)=WSRA(G,G)+NL(G)+WSRC(G)+XXLA*WSRFV(G)
      CALL LSS(IGM,1,IGMD,WSRA,WSQ,DUMY,DET)
      TP=T  $  T=0.0
      DO 310 G=1,IGM
  310 T=T+WSFSS(G)*WSF(G)
      TA=1./T  $  XXLAR=XXLA  $  XXLA=XXLAR-TA
      DO 312 G=1,IGM
  312 WSF(G)=TA*WSF(G)
      IF(ABS(1.-XXLA/XXLAR).GT.EPSO) GO TO 300
C
C
C     EIGENVALUE ITERATION CONVERGED, SCALE FLUX MOMENTS
C     CHOOSE BIGGEST INCREASE IN ALPHA AS BEST NEXT GUESS              10
      IF(ABS(XLA-ALFA).GE.ABS(XXLA-ALFA)) ALFAN=XLA
      IF(ABS(XXLA-ALFA).GT.ABS(XLA-ALFA)) ALFAN=XXLA
      DO 130 L=1,LM $ DO 130 K=1,KM  $  KL=(L-1)*KM+K  $  MAT=IM(K,L)+1
      DO 130 G=1,IGM  $  DO 130 N=1,NM
  130 FLUX(N,KL,G)=F(MAT)*WSF(G)*FLUX(N,KL,G)
  150 RETURN
      END
```

The code blocks in the preceding listing perform the following functions:

Block 1: At the completion of the last outer iteration, the outer rebalance factors [left over in array F(k)] contain the factor $1/\lambda$, in order to maintain a fission total of unity. Loop 18 scales the group-summed flow array (FLGS) by the factors to make them compatible with the already scaled flux (FLUX) and fission source (FISSA) array. Loop 19 does the same scaling to the groupwise net leakage (NL) array, using the factor λ (ALA).

Block 2: The volume-integrated fission source on the material mesh is accumulated.

Block 3: The volume-integrated absorption ABSP (without the α/v_g term) and the total neutrons FV on the material mesh are calculated. Loop 30 cycles over all KM*LM Lagrangian mesh cells, computing the material I.D. (MAT) for each cell. Loop 28 cycles over the 18 possible isotopes for each material. If the isotopic fraction (FR) is nonzero, it computes the cross-section block I.D. (IX) and the total atoms of that isotope (ATOMS) in the cell, based on the total atoms of all isotopes (ANO) in that cell.

Block 4: If there is only one material zone (whole system rebalance), the next α guess (XLA) can be computed explicitly without the inverse power iteration. This equation is equivalent to Eq. (15). The rebalance factor is automatically unity, from the normalization.

Block 5: This block is used for multimaterial rebalance, using the inverse power iteration to solve the rebalance Eq. (8). The α eigenvalue guess (XLA) is set to a large number (10.0 in this case) so the iteration will converge to the eigenvalue of Eq. (8) nearest this value, presumably the desired most positive one. The units of α are here assumed in inverse shakes. If velocities are in cm/s, then this value should be changed from 10 to 10^9. Loop 90 computes the system fission total (T) at the start of the inverse power iteration and the initial guess of the rebalance factors set to this value. Loop 100 is the actual inverse power iteration loop.

Following Wachspress,[16], the power iteration for the eigenvalue equation

$$Mf = \alpha f \qquad \text{(A-1)}$$

is given by

$$f^{n+1} = M^{-1}\alpha^n f^n \qquad \text{(A-2a)}$$

and

$$\alpha^{n+1} = (1,f^n)/(1,f^{n+1}) \quad , \qquad \text{(A-2b)}$$

where n is the power iteration index and (1,f) simply represents the inner product of the vector f with the vector of ones. This simple power iteration converges to the α eigenvalue that is largest in magnitude (positive or negative), which is not the one we desire.

If we have some estimate of the eigenvalue, α_e, Eq. (A-1) may be written

$$(M - \alpha_e I)\, f = (\alpha - \alpha_e)\quad f. \qquad \text{(A-3)}$$

The fractional power iteration is then given by

$$f^{n+1} = (M - \alpha_e I)^{-1}(\alpha - \alpha_e)^n f^n \qquad \text{(A-4a)}$$

and

$$(\alpha - \alpha_e)^{n+1} = (1,f^n)/(1,f^{n+1}) \quad . \qquad \text{(A-4b)}$$

This fractional power iteration will converge to the eigenvalue closest to the guess α_e. If we choose α_e as a large positive number, this will converge to the desired, most positive, α eigenvalue. This iteration is the one coded in Loop 100. In Eq. (A-4), the normalization is (1,f) = 1. In the coding of Loop 100, the normalization is (FSS,f) = 1, in order to maintain a fission total of unity.

Loop 104 constructs the matrix

$$RA = FL + AB - FS + \alpha^n FV \qquad \text{(A-5)}$$

of Eq. (8), where in the above notation,

$$M = FL + AB - FS \quad , \tag{A-6}$$

and the vector on the right-hand side of Eq. (8)

$$Q = FV^* F \quad . \tag{A-7}$$

The call to subroutine LSS solves the inverse matrix equation

$$(M - \alpha_e I)^{-1}(\alpha - \alpha_e)^n f^n$$

of Eq. (A-4a).

Loop 110 calculates a new fission total (T), saving the previous fission total (TP), which is, in fact, 1.0, by the normalization. The next estimate of $(\alpha - \alpha_e)^{n+1}$ in Eq. (A-4b) is then given by

$$(\alpha - \alpha_e)^{n+1} = TA = TP/T = 1.0/T \quad . \tag{A-8}$$

The next iteration estimate, α_e, is then set to the previous iteration's eigenvalue

$$\alpha_e = XLAR \quad , \tag{A-9}$$

and the new iteration's eigenvalue of Eq. (A-4b) is then

$$\alpha^{n+1} = \alpha_e + TP/T = \alpha_e + 1/T \quad . \tag{A-10}$$

Loop 112 then normalizes the rebalance factors f so the fission total T is again unity. The iteration is then terminated when $(1 - \alpha^{n+1}/\alpha^n) < \varepsilon_0$.

Block 6: This block initializes the whole-system rebalance (WSGR) arrays to zero.

Block 7: This block accumulates the WSGR arrays C (or WSRC), FV (or WSRFV), S (or WSRS), and the first row of array FS (or WSRFS), as given in Eq. (21).

Block 8: Loop 220 stores the groupwise whole system fission source, the first row of the FS array, into the WSFSS array, to be used later in the normalization constraint. Loop 210 fills out the remaining rows of the FS array. Loop 212 then multiplies the FS array by the χ diagonal matrix to obtain the final form of FS, as given in Eq. (21e). The WSGR α estimate (XXLA) is set to a large number (10.0), the fission total (T) again computed, and the initial guess of the rebalance factors equated to this value.

Block 9: Loop 300 is the inverse power iteration for the WSGR equations, virtually identical to the coding of Loop 100, except the WSGR arrays are used.

Block 10: The next guess of the α eigenvalue (ALFAN) is chosen between the GCCMR estimate (XLA) and the WSGR estimate (XXLA) in order to maximize the change from the previous α eigenvalue estimate (ALFA). Loop 130 then applies the GCCMR factors (F) and the WSGR factors (WSF) to the scalar flux and moments. Both rebalance factors are normalized to maintain the fission total of unity.

REFERENCES

1. T. R. Hill, "ONETRAN, A Discrete Ordinates Finite Element Code for Solution of the One-Dimensional Multigroup Transport Equation," Los Alamos Scientific Laboratory report LA-5990-MS (June 1975).

2. R. D. O'Dell, F. W. Brinkley, Jr., and D. R. Marr, "User's Manual for ONEDANT: A Code Package for One-Dimensional, Diffusion-Accelerated, Neutral-Particle Transport," Los Alamos National Laboratory report LA-9184-M (February 1982).

3. K. D. Lathrop and F. W. Brinkley, Jr., "TWOTRAN-II: An Interfaced, Exportable Version of the TWOTRAN Code for Two-Dimensional Transport," Los Alamos Scientific Laboratory report LA-4848-MS (July 1973).

4. W. W. Engle, Jr., "A User's Manual for ANISN, a One-Dimensional Discrete Ordinates Transport Code with Anisotropic Scattering," Union Carbide Corporation report K-1693 (March 1967).

5. W. A. Rhoades and R. L. Childs, "An Updated Version of the DOT 4 One- and Two-Dimensional Neutron/Photon Transport Code," Oak Ridge National Laboratory report ORNL-5851 (July 1982).

6. G. I. Bell and S. Glasstone, Nuclear Reactor Theory (Van Nostrand Reinhold Co., New York, 1970).

7. G. Milton Wing, An Introduction to Transport Theory (John Wiley & Sons Inc., New York, 1962).

8. M. M. R. Williams, The Slowing Down and Thermalization of Neutrons (John Wiley & Sons Inc., New York, 1966).

9. E. W. Larsen and P. F. Zweifel, "On the Spectrum of the Linear Transport Operator," J. Math. Phys., 15 (11), 1987 (1974).

10. E. W. Larsen, "The Spectrum of the Multigroup Neutron Transport Operator for Bounded Spatial Domains," J. Math. Phys. 20, 8, 1776 (1979).

11. J. J. Duderstadt and W. R. Martin, Transport Theory (John Wiley & Sons Inc., New York, 1979).

12. B. G. Carlson and K. D. Lathrop, "Transport Theory-The Method of Discrete-Ordinates," in Computing Methods in Reactor Physics, H. Greenspan, C. N. Kelber, and D. Okrent, Eds. (Gordon and Beach, New York, 1968).

13. R. Mohan, F. Ahmed, and L. S. Kothari, "Decay of Fast Neutron Pulses in Uranium Assemblies," Nucl. Sci. Eng. 81, 532 (1982).

14. T. R. Hill and R. R. Paternoster, "Two-Dimensional Spatial Discretization Methods on a Lagrangian Mesh," Los Alamos National Laboratory document LA-UR-82-1055 (April 1982).

15. E. W. Larsen in "Transport and Reactor Theory, July 1 - September 1982," R. D. O'Dell and R. E. Alcouffe, Los Alamos National Laboratory report, in preparation.

16. E. L. Wachspress, Iterative Solution of Elliptic Systems (Prentice-Hall, Englewood Cliffs, New Jersey, 1966).

17. G. R. Keepin, Physics of Nuclear Kinetics (Addison-Wesley, Reading, Maine, 1965).

18. Y. Mingzhu and Z. Guangtian, "Spectrum of Neutron Transport Operator with Anisotropic Scattering and Fission," Scientia Sinica 24, 476 (1981).

19. I. Marek, "On the Asymptotic Behavior of Solutions of the Homogeneous Transport Equation," in Differential Equations and Numerical Mathematics: Selected Papers Presented to a National Conference, G. I. Marchuk, Ed. (Novosibirsk, USSR 1978).

☆U.S. GOVERNMENT PRINTING OFFICE: 1983-0-676-026/17

Printed in the United States of America
Available from
National Technical Information Service
US Department of Commerce
5285 Port Royal Road
Springfield, VA 22161

Microfiche (A01)

Page Range	NTIS Price Code	Page Range	NTIS Price Code	Page Range	NTIS Price Code	Page Range	NTIS Price Code
001-025	A02	151-175	A08	301-325	A14	451-475	A20
026-050	A03	176-200	A09	326-350	A15	476-500	A21
051-075	A04	201-225	A10	351-375	A16	501-525	A22
076-100	A05	226-250	A11	376-400	A17	526-550	A23
101-125	A06	251-275	A12	401-425	A18	551-575	A24
126-150	A07	276-300	A13	426-450	A19	576-600	A25
						601-up*	A99

*Contact NTIS for a price quote.

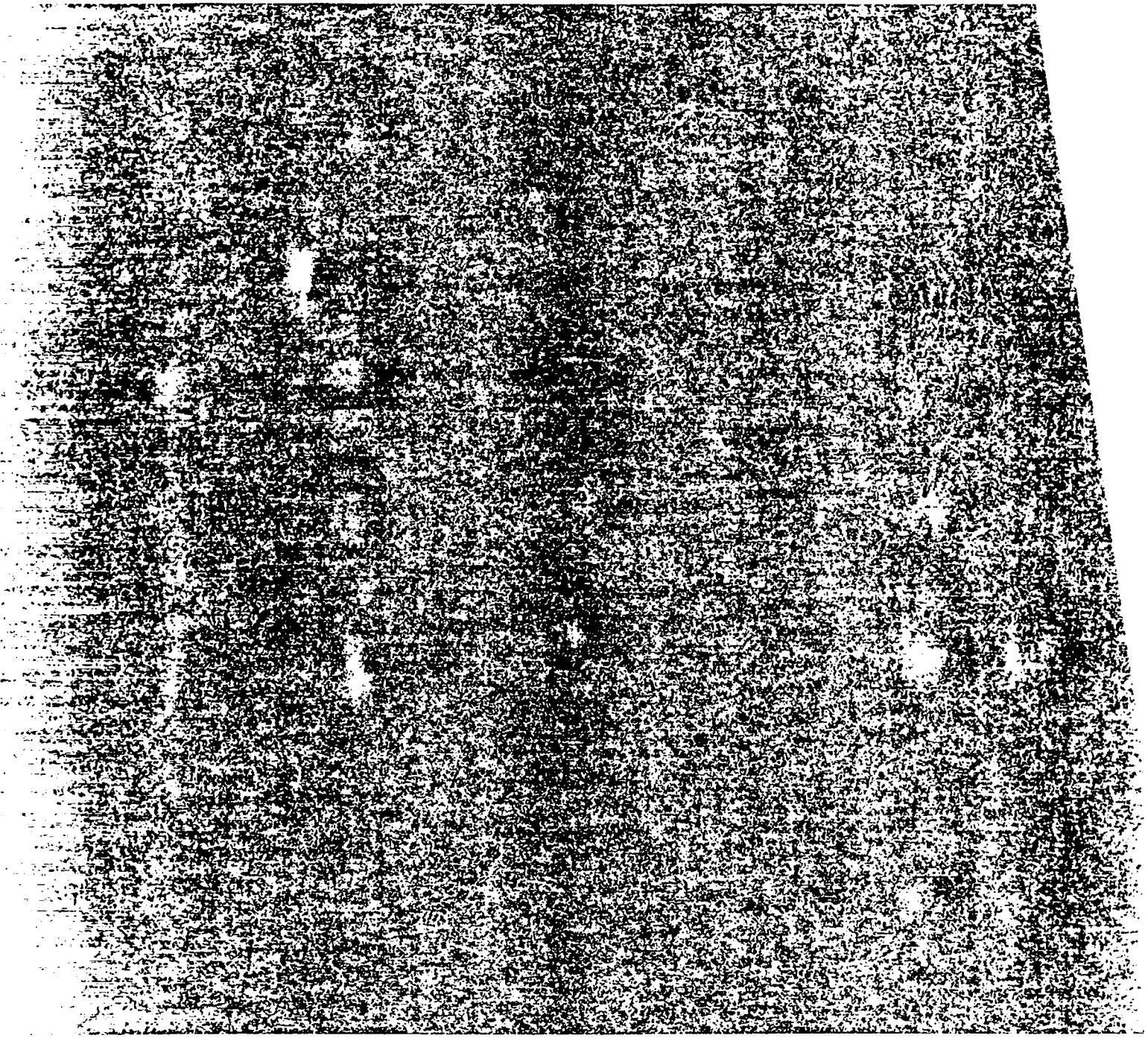

Los Alamos